APPLICATIONS OF TWIST BONDING

A Thesis

Presented to the Faculty of the Graduate School

of Cornell University

in Partial Fulfillment of the Requirements for the Degree of

Master of Science

by

Ryan Peter DiSabella

January 2007

ABSTRACT

Two processes have been developed by which twist boundaries may have useful application. The first of these, the compliant universal substrate, attempts to utilize a twist boundary to allow the growth of large lattice mismatch, low defect density heteroepitaxial layers. The second, the periodic template, attempts to use the periodic stress fields inherent in a twist boundary to produce two-dimensional surface topography with a very fine, and controllable, periodicity.

One sample of germanium grown on a silicon compliant substrate was analyzed in a JEOL 1200EX transmission electron microscope. The analysis showed that the twist boundary was not present in all regions of the Si-Ge interface. In those regions where the twist-bonded layer was observed, it was established that the Ge crystal was rotated approximately 45° from the underlying bulk Si wafer. In those regions where the layer was not present, no such rotation was observed. Due to the small size of the domains in which the compliant layer was present or absent, strong conclusions with respect to its effect on defect densities can not be drawn. High magnification investigations of the twist bonded layer showed that it does exhibit a roughly periodic internal structure.

Attempts were made to fabricate periodic templates with silicon, gallium arsenide, and gold bicrystals. Twist bonding of gold proved to be the most successful of the three materials. Gold films were sputtered epitaxially onto sodium chloride crystals at 450° C and subsequently annealed for one hour at 600° C. Two films, one approximately 500 nm thick and one

approximately 20 nm thick, were bonded together in a hot press at ~1.0 MPa at 300° C for 1.2 hours. The misorientation angles of these bicrystals were kept below 5° to maintain a reasonable dislocation spacing. The bicrystals were then characterized using the JEOL 1200EX TEM and a Nanaoscope III atomic force microscope. Small amplitude surface modulations whose periodicity matched that of the underlying dislocation structure were observed.

BIOGRAPHICAL SKETCH

Ryan DiSabella was born on March 30, 1973 in Easton, Pennsylvania. His family settled in their current home in Mountain Top, Pennsylvania in 1977. Ryan attended public schools in the Hazleton area, where he met one Tiffiny Lynn, whom he married in August of 1998.

Ryan carried out his undergraduate studies at the University of Pittsburgh, where he earned degrees in Materials Science Engineering and Interdisciplinary Studies, with concentrations in Philosophy and Italian Studies. In August of 1996 he began his graduate studies in the department of Materials Science and Engineering at Cornell University. He has since been employed in the steel industry working in a variety of technical capacities, and is currently a member of the Research and Development staff at Carpenter Technology Corporation.

To my wife and to my parents

ACKNOWLEDGMENTS

I would like to thank my advisor, Prof. Stephen L. Sass, for his guidance, support, and encouragement throughout all of the various projects that I was involved with during my stay at Cornell. Without his mix of vision, optimism, and healthy skepticism none of this work could have been accomplished. Additionally, through both coursework and practical assistance, Prof. Sass taught me more about transmission electron microscopy then I had imagined possible. I would also like to thank my two minor advisors, Prof. Yu-Hwa Lo and Prof. Frank J. DiSalvo. Professor Lo's idea that the twist boundary may actually have useful application in solving material problems was the wellspring from which all of this work developed. His guidance and advice were both appreciated. Professor DiSalvo's advisement provided this work with new insights into problems that I had overlooked or found intractable.

The support staff of both the MSC and Materials Science laboratories provided me with a great deal of assistance, and deserve all due thanks. I would like to thank John Hunt and Gerhard Schmidt of the MSC, for their assistance with the TEM and the AFM, respectively. I would like to thank John Sinnott, who at the time was working in the Materials Science and Engineering department, for all his assistance with hot presses, machine tools, and mechanical design. I would like also like to thank Peter Revesz and Nick Szabo, for their assistance with RBS characterization, and Maura Weathers for her assistance in the X-ray diffraction laboratories.

There are a large number of students, graduate and undergraduate, who have been influential in the completion of this work. Dr. Zhenjun Zhang,

Dr. Jeff Smith, and Dr. Shanthi Subramanian all helped to teach me how to carry out scientific research. I would particularly like to thank Drs. Smith and Subramanian for their advisement and encouragement. Current Sass group members Tom Barbieri, Martin Murtagh, and Andrew Darlak all deserve my gratitude. Tom has been a true friend, Marty helped to keep the office interesting and less pessimistic, and Drew has taken what I began to new levels. Kirvan Laura Chao, Linnea Hartsuyker, Su Kim, and Panitarn Wanakamol all managed to produce interesting and helpful results despite my absolute dearth of managerial skills. I would also like to thank several members of the Lo group, Dave Crouse, Srivatsa Lakshmi, and Rong Zhou, for providing me with samples of the compliant substrate and assisting in my own sample preparation.

Lastly, I would like to thank my wife, Tiffiny, and my family. My family's support over these years of schooling was more than could have been asked for. Without the patience, understanding, and love that Tiffiny has shown me, I never would have made it to this point.

TABLE OF CONTENTS

LIST OF TABLES

LIST OF FIGURES

CHAPTER ONE:
INTRODUCTION

A twist boundary is a grain boundary between two crystals which have the same surface normal and are rotated with respect to one another about this normal. Such structures have long been a subject of interest, typically as model systems to gain insight into the properties of general grain boundaries. Since most effects associated with grain boundaries are detrimental to material properties, e.g. grain boundary embrittlement, reduced creep resistance, stress corrosion cracking problems, etc., practical applications of bicrystals containing twist boundaries were never envisioned. However, recent research has determined that such structures may actually be useful in several applications. Work done at Cornell University has established a method by which defect-free heteroepitaxial layers of large lattice mismatch may be produced.[1] The key feature of this compliant universal substrate (CUS) process, is the use of a bicrystal containing a large angle twist boundary. It has also been postulated that the periodic stress field associated with a twist boundary may be used to produce a periodic template, a crystal with a two-dimensionally periodic surface topography in a suitable bicrystal. Such a template can, in principle, have spacings ranging from a few nanometers to several tens of nanometers, all by varying the misorientation angle. This chapter shall describe some of the general properties of twist boundaries, most notably the stress and strain fields associated with them. Then the concept of compliant substrates shall be considered with a particular emphasis on the concepts behind and the prior results of the CUS process. Finally, the creation

of periodic surfaces through the use of bicrystals containing twist boundaries shall be addressed.

1.1 SMALL-ANGLE GRAIN BOUNDARIES

The process of forming a grain boundary will result in a fairly uniform high misfit between the two lattices along the boundary plane if structural relaxation does not occur. Most material systems relax into a lower energy structure consisting of regions of both high and low misfit. Both the unrelaxed and relaxed configurations of a twist boundary where the misorientation axis is [001] are depicted in **Figure 1**. As can be seen, the relaxation results in a periodic grain boundary structure. The regions of high misfit are actually screw dislocations. Due to the regular arrangement of these dislocations, their strain fields interact with one another such that this boundary is actually a relatively low energy structure.

Figure 2 shows a bright field image of a θ=3.4° twist boundary contained in a gold bicrystal. A square array of dislocations is present. The dislocation spacing in this image is ~5 nm. For small-angle boundaries, the dislocation spacing is determined by Frank's Rule:

$$\mathbf{d} = \mathbf{b}/\theta \qquad (1.1)$$

while the general equation is:

$$2\mathbf{d} = \mathbf{b}/\sin(\theta/2) \qquad (1.2)$$

Table 1 shows the dislocation spacings, as calculated by Frank's Rule, for twist boundaries of various misorientation angles in gold, silicon, and GaAs. For all materials it is assumed that the Burgers' vectors of the screw dislocations are of the form $\mathbf{a}/2$ [110], giving $|\mathbf{b}|$=2.89Å for gold, $|\mathbf{b}|$=3.84Å for silicon, and $|\mathbf{b}|$= 4.00Å for GaAs.

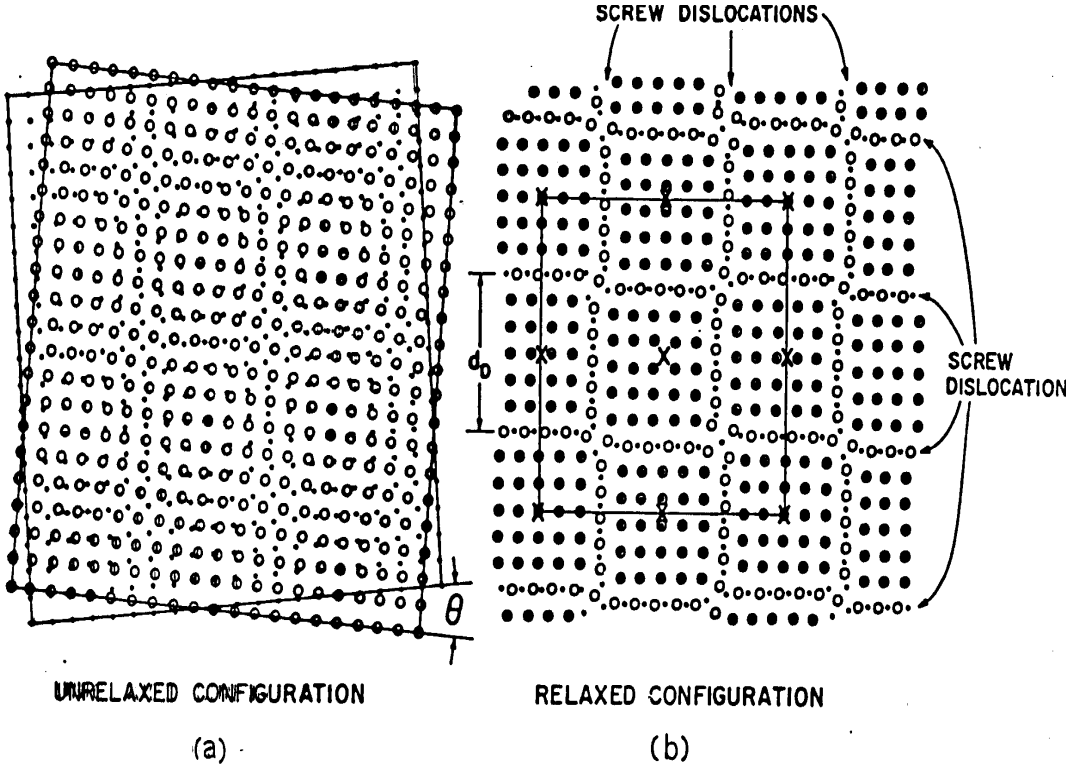

Figure 1: Atomic positions in the planes above and below a twist boundary in both the a)unrelaxed and b) relaxed configurations

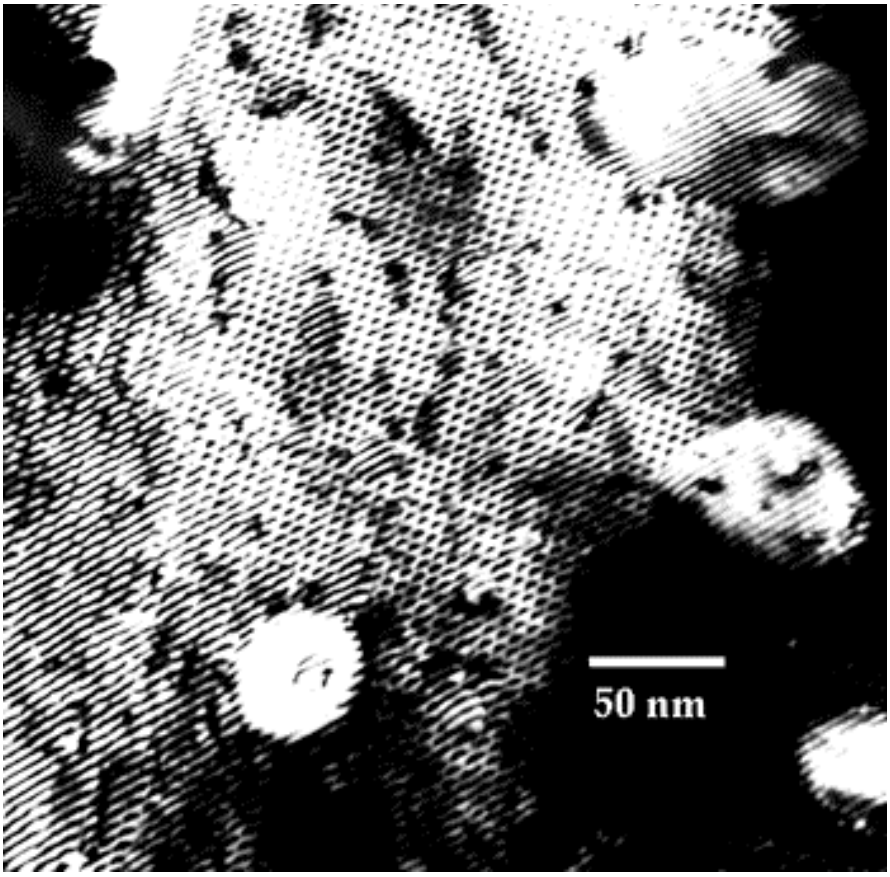

Figure 2: Bright-field image of a 3.5° twist boundary in Au

TABLE 1.1:

DISLOCATION SPACINGS IN [001] TWIST BOUNDARIES

	$d_{dislocation}$ (nm)		
Theta (°)	Au	Si	GaAs
0.25°	66.1	88.0	91.6
0.5°	33.0	44.0	45.8
1.0°	16.5	22.0	22.9
2.0°	8.26	11.1	11.9
5.0°	3.31	4.41	4.59
10.0°	1.66	2.21	2.30
20.0°	0.84	1.12	1.17
45.0°	0.41	0.54	0.57

At high angles, the dislocation spacing becomes so small that the dislocation cores begin overlapping. At such angles, Frank's Rule no longer accurately describes the boundary structure. The CUS process utilizes bicrystals containing such high angle boundaries for the growth of low defect-density heteroepitaxial films.

Hirth and Lothe give the following equation for the stress field associated with a single screw dislocation[2]:

$$\tau_r = \mu \mathbf{b} / 2\pi r \qquad (1.3)$$

where μ is the shear modulus, **b** is the Burgers vector, ν is Poissons ratio, and r is the radial distance form the dislocation core. To be rigorously valid, the above equation should account for the dimension of the dislocation core in which the material can not be treated as an elastic continuum. However, such a correction is typically inconsequential at distances more than a few

nanometers from the dislocation. Hirth and Lothe also show that the stress field associated with an edge dislocation is:

$$\tau_{xy} = \mu \mathbf{b} / 2\pi(1-\nu) * y(3x^2 + y^2) / (x^2 + y^2)^2 \qquad (1.4)$$

where μ and **b** are as above, ν is Poissons ratio, and x and y are positional coordinates with respect to the dislocation core. The stress field of a tilt boundary, which can be represented as a series of edge dislocations with spacing d, is calculated by Hirth and Lothe as a superposition of the stress fields from an infinite series of edge dislocations[2]. The resultant stress field is:

$$\tau_{xy} = \mu \mathbf{b} / 2(1-\nu) d^2 * \pi x / (\sinh^2(\pi x / d)) \qquad (1.5)$$

Figure 3 shows the stress field of a 2.0° tilt boundary in gold and that of a single edge dislocation in the same media as a function of distance from the boundary. As can be seen from this figure, the stress associated with a small angle grain boundary is significantly less than that of a single dislocation at any appreciable distance from the boundary plane. As a first order approximation for small angle twist boundaries, the stresses can be assumed to be lower than the critical resolved shear stress for any distance from the boundary greater than the dislocation spacing, d.

One other key property of twist boundaries is their activity as impurity gettering sites. It has long been known that grain boundaries serve as low energy sites for impurities and even precipitation of second phases.[3] Though twist boundaries contain low energy dislocation structures, their internal energy is much higher than that of the surrounding perfect crystal lattice. As such they serve as very favorable sites for impurity atoms and second phase residence. Several studies have been carried out on segregation and precipitation at Si and GaAs grain boundaries.[4-6] Goessele *et. al.* have determined that, for boundaries with misorientations of greater than ~5°,

bonds of Czochralski wafers will form an interfacial oxide in lieu of a twist boundary, while float-zone refined wafers form no such oxide.[7]

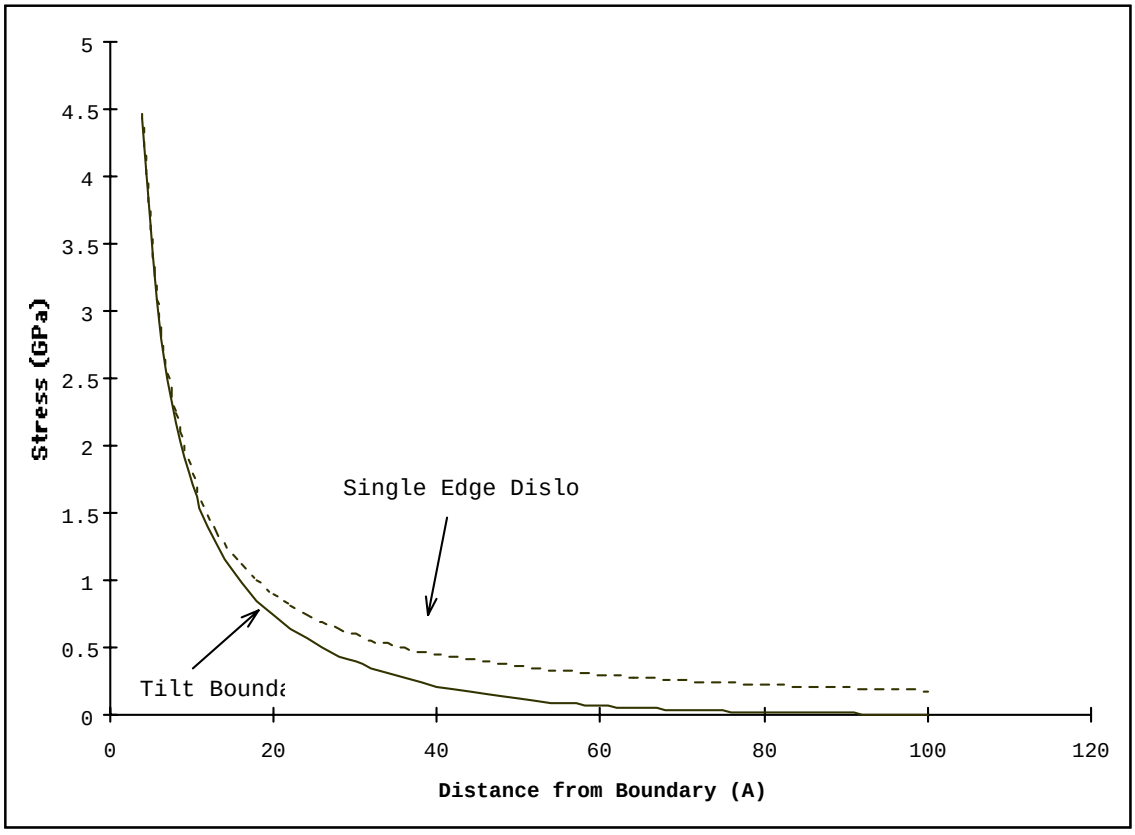

Figure 3: Comparison of the stress field of a tilt boundary and a single edge dislocation

1.1.1 Stress and Energy Fields at Twist Boundaries

In 1949 Van der Merwe analyzed the energy a boundary between two crystals rotated with respect to another about a common axis.[8] His analysis utilized the technique developed by Peierls and Nabarro.[9-10] The derivation is based upon the following reasoning. Take a crystal and slice it into two halves. "Turn off" the interatomic potentials at the interface of the two half-crystals and rotate each by $\theta/2$ in opposite directions. Now "turn on" the interatomic potentials at the interface and calculate the resultant shear stresses and energies. The key assumptions in this derivation are those first used by Peierls and Nabarro: 1) Reasonably far from the interface, each half crystal can treated as an elastic continuum, and 2) The interatomic potentials are described by a simple sinusoidal force law. Hence, the relevant energies at a twist boundary are those of the interatomic potential attempting to restore the system to a 'non-twisted' configuration and those of the elastic media which resist this restoring force.

The details of this derivation are long and complex; the interested reader is referred to the original papers by van der Merwe and related papers by Nabarro and Herring.[8-12] The key result of the twist boundary analysis are a number of equations describing the shear stress and displacements caused by the presence of the dislocation network. The expressions that van der Merwe arrives at for τ_{xy} and τ_{zy} are quite complicated and involve a number of Fourier Series. However, the primary concern of the current research is effect of the twist angle on these stress fields and the rapidity with which they fall

off as one moves away from the interface. Given these interests, one can simplify the van der Merwe expressions to the following:

$$\boldsymbol{\tau}_{xy} = P\{\cos(2\pi x/d) - A\exp(-2\pi z/d)\}\exp(2\pi z/d) \quad (1.6)$$

$$\boldsymbol{\tau}_{zy} = -P \sin(2\pi x/d) \exp(-2\pi z/d) \quad (1.7)$$

Where x is the distance along the plane of the boundary, z is distance perpendicular to the boundary, P is a constant prefactor which is an assemblage of material and geometrical parameters, A is a Fourier coefficent (which is constant for any given misorientation), and d is the dislocation spacing as determined by Frank's Rule.

Figure 4 and **Figure 5** depict the variation in τ_{xy} and τ_{zy}, respectively, as one moves along the boundary in x and away from it in z. To keep matters simple, the stresses are plotted normalized with respect to the magnitude of the prefactor and A is assumed to be equal to 2. A dislocation spacing of 28 Å was assumed, this is equivalent to a gold boundary with a spacing of 10**b**. The periodic variation of the stress field in the x direction is obvious. The period of this variation is equivalent to that of the dislocations themselves. Additionally, the magnitude of these stresses falls rapidly, more rapidly than z^{-1}, with distance from the boundary. This is in agreement with the stress state depicted in **Figure 3** and with the argument that the regular dislocation networks of small angle grain boundaries result in stress and strain fields that are localized to the vicinity of the interface.

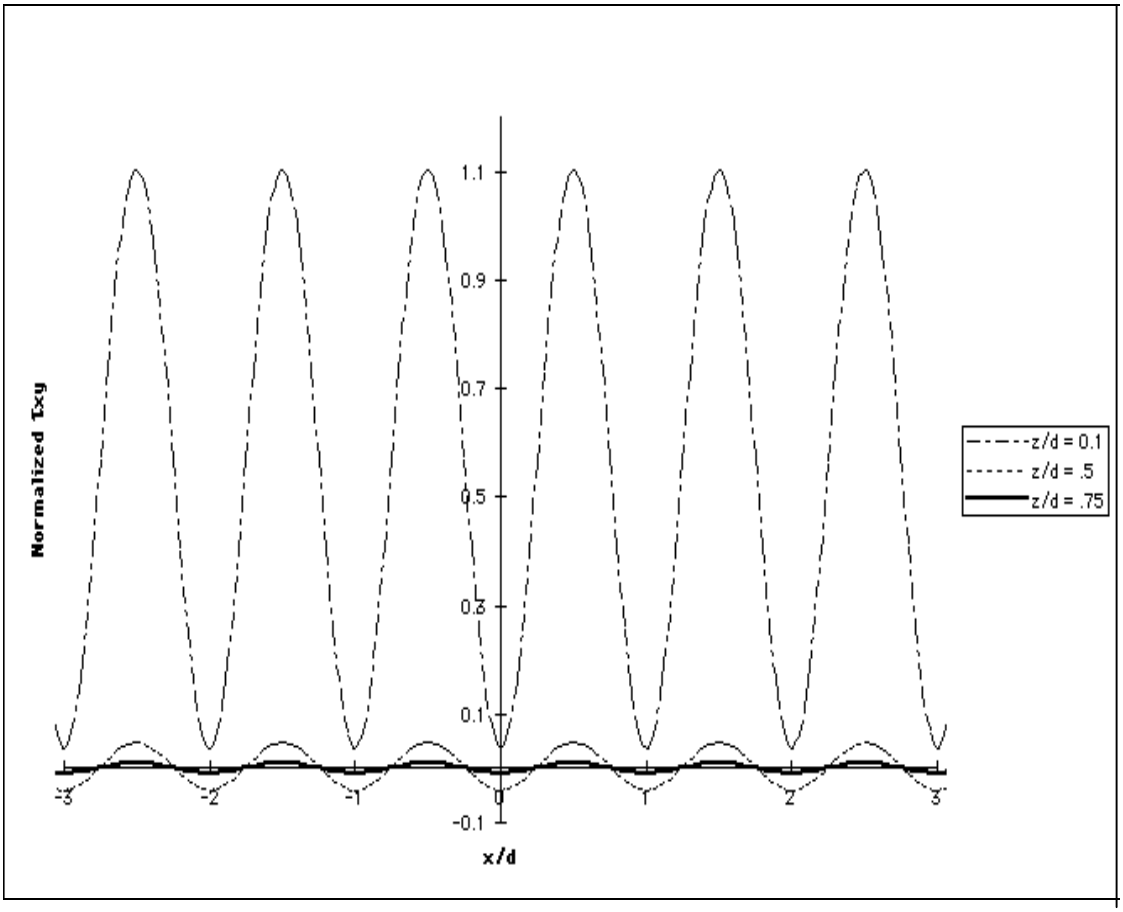

Figure 4: τ_{xy} as a function of distance along and away from twist boundary

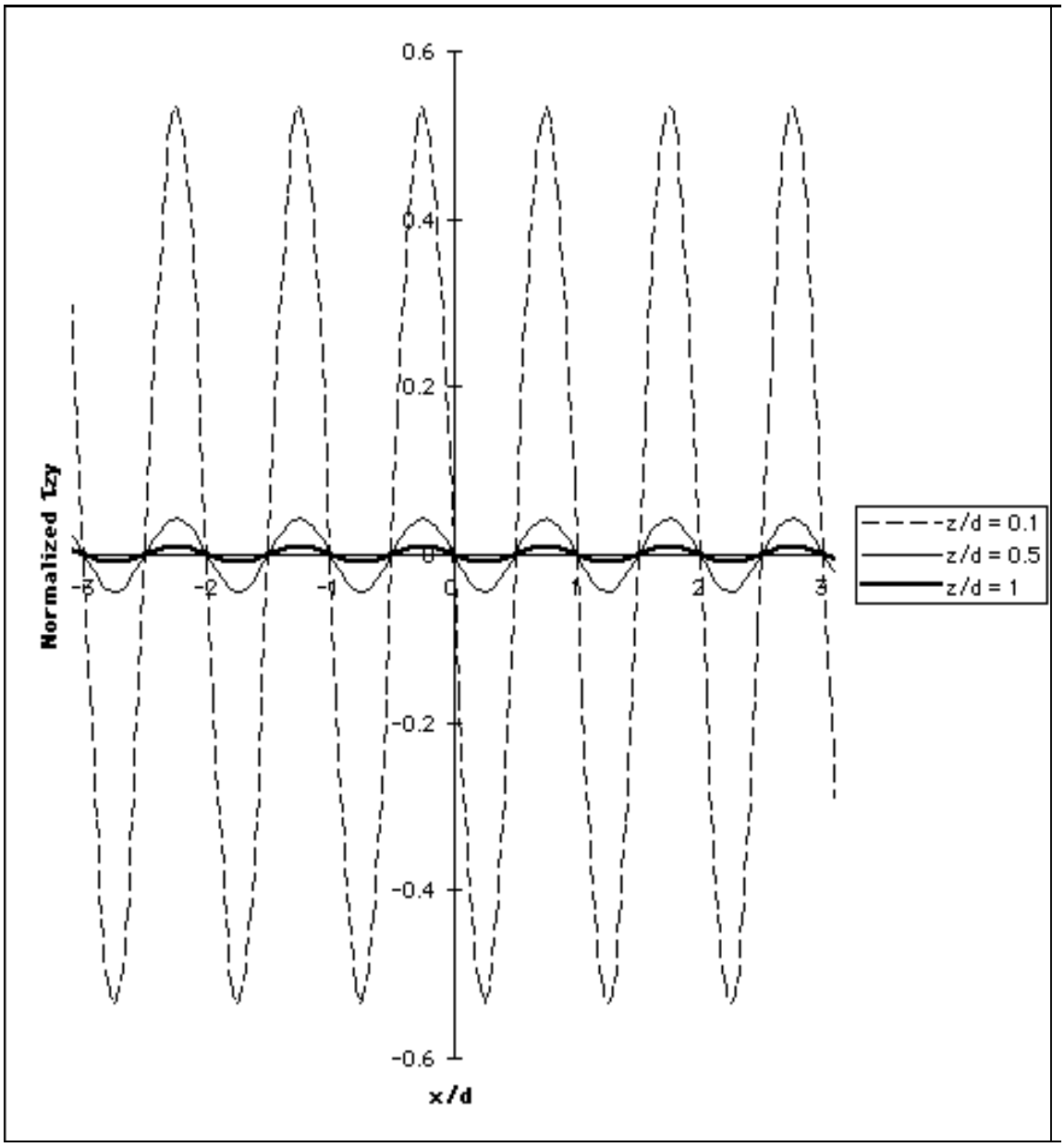

Figure 5: τ_{zy} as a function of distance along and away from twist boundary

1.2 COMPLIANT SUBSTRATES

The "tuning", or optimization, of material properties with respect to their application is one of the most important methods by which technology advances. The field of semiconductor electronics, in particular semiconductor optoelectronics, is one in which some of the most important strides forward have arisen from such materials optimization. The ability to create a continuum of band gap energies from which one can select the gap most appropriate for the application at hand has been a topic of considerable interest. Such an ability would be of immense value in the area of semiconductor optoelectronics, as this would allow for the production of light at any wavelength desired, e.g., for the production of a laser operating in the blue-green region of the spectrum.

The development of growth techniques such as molecular beam epitaxy (MBE) and metal-organic chemical vapor deposition (MOCVD) has allowed for the production of many novel semiconducting compounds and thereby, production of materials with novel properties. Through the use of alloying of III-V semiconductor materials, the desired continuum of band gap energies can be achieved. **Figure 6** depicts the band gap energy as a function of the lattice constant of the material.[13] Novel band gaps can be produced via alloying of multiple III-V compounds. The lattice constant of such an alloy is calculated following a rule of mixtures:

$$\mathbf{a_o}(A_{1-x}B_xC) = \mathbf{a_o}(AC) - x\mathbf{a_o}(BC) \qquad (1.8)$$

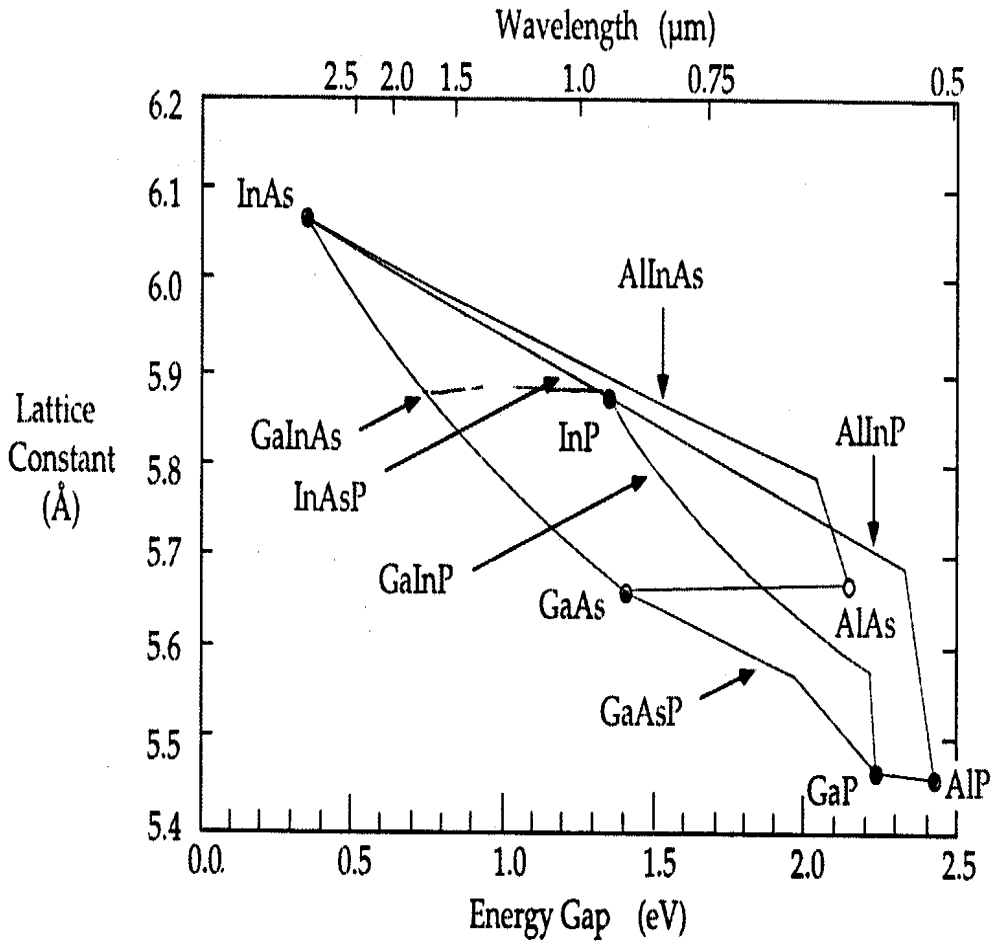

Figure 6: Band gap energies and lattice constants for III-Vcompounds and alloys (Figure courtesy of R. Sheally)

where A, B, and C are the elemenatal components of the alloy, a_o is the lattice constant, and x is the mole fraction of the binary component of the alloy. The variation of the band gap energy tends to follow a more complex functionality than that of the lattice constant and is subject to the particularities of the band diagram of each of alloying compounds.

From the information on **Figure 6**, it would appear that the problem is solved and that one can produce a material of the desired band gap energy for any application. However, although one can in principle obtain a material of almost any bandgap, in practice the quantity and quality that can be produced remains quite limited. The key to this is in the ordinate of **Figure 6**, the lattice constant. As one varies the band gap of a semiconductor through alloying there is a concomitant variation in the lattice constant. When one attempts to epitaxially grow a film of one lattice constant on top of a substrate of a different lattice constant, a strain equal to the lattice mismatch will develop. This strain develops not only during the growth of alloyed materials, but also in heteroepitaxial growths, i.e., the growth of a completely different material on top of a substrate material.

This strain, and its associated stress, are typically relieved through the formation of crystal defects, most noticeably dislocations. These dislocations can penetrate throughout the whole of the growth layer. Such dislocations are referred to as 'threading' dislocations, and cause serious problems with device performance. These threading dislocations serve as electronic defects, acting as traps or recombination sites, and lead to strong degradation of optical properties.[14]

It has been experimentally found that these threading dislocations only form after a certain critical thickness for the heteroepitaxial layer has been

surpassed. Below this thickness, the film is able to elastically accommodate the stresses generated by the lattice mismatch. Early work by van der Merwe analyzed the formation of defects at interfaces in general, in addition to the twist boundaries discussed earlier.[8] He utilized a similar analysis taking the Peirels-Nabarro model of a dislocation and the strain energy of the lattice mismatch to calculate both the interfacial energy of a heteroepitaxial boundary and an approximate expression for the thickness at which dislocations will begin to form. This work was further refined by Matthews and Blakeslee to derive an analytical expression for the critical thickness.[15]. In their analysis, the growing epitaxial film would be elastically strained to maintain coherence until a thickness was reached where it was energetically favorable to accommodate the lattice mismatch through the formation of dislocations as opposed to continued elastic strain. Their derivation resulted in the following expression for the critical thickness of a defect-free heteroepitaxial layer:

$$h_c = (\mu \mathbf{b}/4\pi(1-\nu)Mf)*\ln(h_c/\mathbf{b})$$

where h_c is the critical thickness, ν is Poisson's ratio, M is the biaxial modulus of the film, μ is the shear modulus of the film, and **b** is Burgers vector.

Work by Bean *et al* has shown that the critical thickness of Si-Ge alloy layers on Si as calculated via the Matthews-Blakeslee (M-B) analysis can be exceeded without the formation of threading dislocations.[16] Nix[17] and Hagen and Strunk[18] have proposed various models whereby such growth can occur. Nix's models all deal with the kinetic constraints placed upon the propagation of a threading dislocation in a thin film**.** He points out that a dislocation moving through a thin film will have to lay down dislocation line length along the film-substrate or the film-passivation interface which will increase the dislocation's energy of formation. Hence, one would expect a greater critical

thickness than postulated by Matthews and Blakeslee. The work of Bean *et al* supports such a model, since they did find the Si-Ge growths on Si to exhibit a critical thickness for defect formation which was greater than that calculated from the M-B analysis.

Since these ideas were first put forth, many researchers have attempted to overcome the critical thickness limit defined by Matthews and Blakeslee. One of the methods investigated has been wafer bonding.[19-21] In this technique, materials of different lattice constant are brought together under conditions of high temperature and pressure with the hope of forming reasonably strong interfacial bonds. Typically, one material will have been grown on a substrate that must be subsequently removed via an etching process. Another method that has been studied is epitaxial liftoff.[22-23] In this technique, the desired material is grown on one substrate, then removed and placed on another. Hopefully, some weak bond, e.g. Van der Waal's or hydrogen, will form between the two materials. The liftoff is accomplished by means as divergent as etching and actual mechanical force. Both techniques exhibit a modest success rate, at best. Additionally, they generally only work for materials for which some approximately lattice matched substrate exists.

Compliant substrate techniques attempt to overcome the Matthews-Blakeslee limitation by creating a more 'forgiving' substrate material. Some method for accommodating the strain energy caused by the lattice mismatch is introduced into the substrate material. Two presently existing technologies for accomplishing this have met with success.[24-25] One approach, whose principal investigators work out of Georgia Tech, has been to use topographically patterned, and hence strain modulated, GaAs wafers. The

other approach, under investigation at Cornell University along with collaborators, has been deemed the Compliant Universal (CU) Substrate.

The CUS approach attempts to create a 'reverse' Matthews-Blakeslee type process. According to the M-B analysis, one can grow a defect-free heteroepitaxial film of any lattice mismatch, provided that one grows the epitaxial layer thin enough What would happen if the substrate was very thin, ~10 nm, and free standing? Ostensibly, one could grow a very thick layer of any material on top of this substrate. Of course, such a substrate would be virtually useless due to its scale: how could it be held? However, what if one could create some layered structure or surface modified substrate that would be so isolated from the rest of the substrate so that it behaves like a free-standing thin layer?

Original efforts to create such a thin layer utilised etching processes to create a thin bridge of GaAs above a conventional substrate.[26] These met with some success, but the scale of this substrate made it too weak to be viable for commercial usage. The current research uses twist wafer bonding to create a thin layer bonded to a conventional substrate which then allows for thick, low defect-density heteroepitaxial growth.[24]

Twist wafer bonding produces a large angle twist boundary between a thin crystal (~100Å) and a conventional wafer by hot pressing two semiconductor wafers together at a large misorientation angle. **Figure 2** presented an image of a small angle twist boundary where the square dislocation grid is easily discernible. At the high angles used in the formation of CU substrates, the dislocation spacing is too small and the contrast is too low for the dislocation network to be resolvable. It was thought that such a high angle twist boundary might be a good way to isolate the behavior of the

thin layer from that of the underlying substrate; thereby producing a compliant substrate.

Figure 7 shows the cross sectional TEM images obtained for the growth of $In_{0.35}Ga_{0.65}P$ on GaAs (1% lattice mismatch) via the CU process.[27] The specimen on the top was grown without a compliant layer while the one on the bottom used a 10 nm compliant layer. The InGaP layer is approximately 30 times the Matthews-Blakeslee critical thickness for such a lattice mismatch. The presence of threading defects is obvious in the material grown without the compliant layer whereas in the CU material there are no discernible dislocations. The region of InGaP on CU substrate shown here is representative of the whole specimen; it was calculated that the dislocation density in this material could be 10^6/cc at most. No dislocations were observed at all in this specimen, and this density is merely a 'worst-case-scenario' number due to the limited field of vision in a TEM.

A much larger lattice mismatch heteroepitaxial growth was next attempted. A 650 nm film of InSb, which is 14.7% compressively mismatched to GaAs, was grown on both a conventional GaAs and a 40 Å CU GaAs substrate. **Figure 8** shows the bright field TEM images obtained from these specimens, again with the conventional substrate on the top

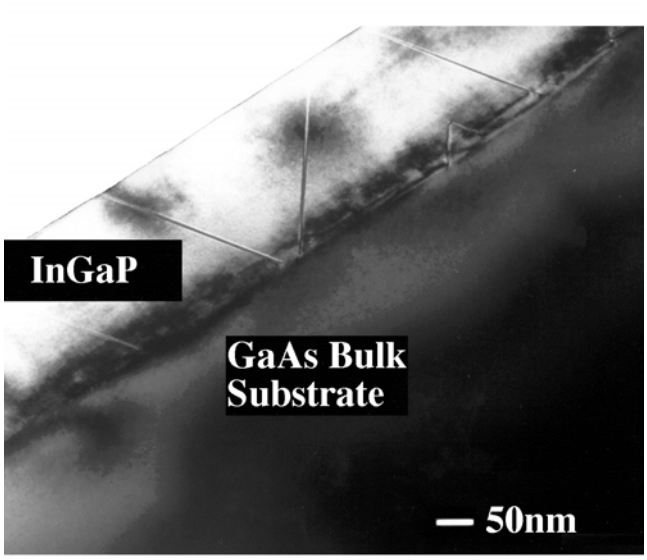

No CU Layer

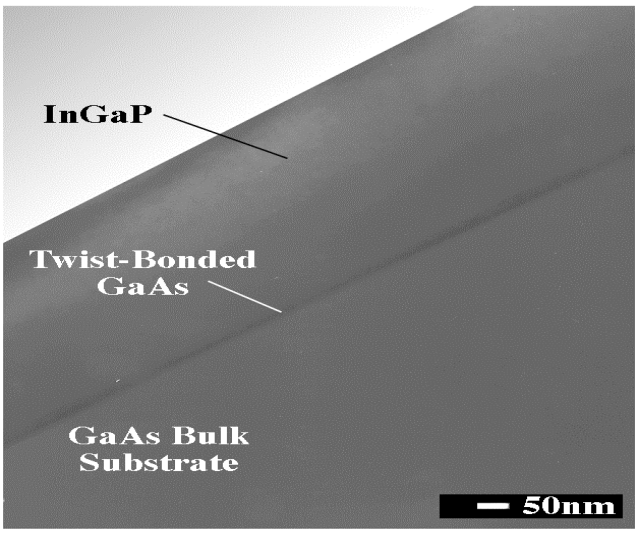

With CU Layer

Figure 7: Growth of InGaP on GaAs

(Micrographs courtesy of F. Ejeckham)

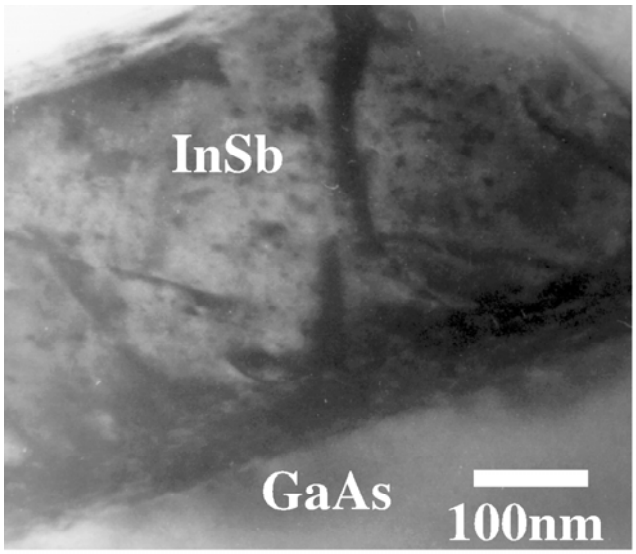

Without CU Layer

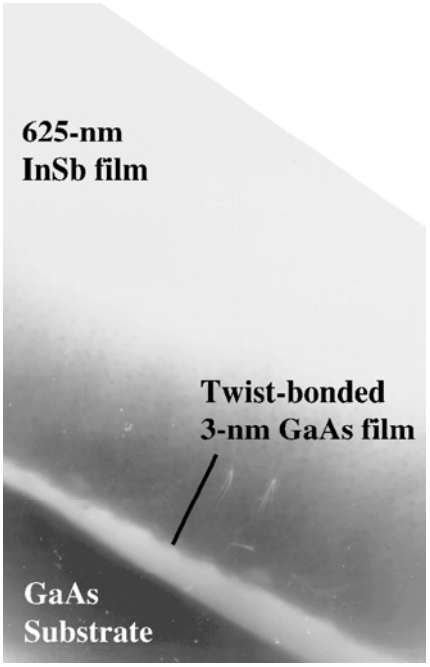

With CU Layer

Figure 8: Heteroepitaxial growths of InSB on GaAs both without and with a twist-bonded compliant layer (Micrographs courtesy of F. Ejeckham)

and the CU substrate on the bottom.[27] The conventional substrate material has an exceedingly high dislocation density, as is evidenced by the large amount of defect contrast visible in the InSb film. On the other hand, the CU substrate material again exhibits no dislocations. Electron diffraction data on both the InSb CU material and the InGaP CU material showed that both epitaxial layers were misoriented with respect to the underlying bulk substrate. Photoluminescence spectra from these materials also exhibited a marked improvement over those grown on the plain GaAs substrate.

Tests were also performed on GaSb layers grown on GaAs CU substrates, an 8% lattice mismatch. **Figure 9** shows a region of the grown crystal.[28] Some small concentration of defects was determined to be present in the specimen, but the number was still much less than that of the layer grown on conventional GaAs. **Figure 10** shows a higher magnification image of the interface region.[28] If one can assume that the thin band of contrast at the interface is the CU layer, then it appears that the layer has undergone localized plastic deformation. Local deformation of the boundary may provide the stress relaxation that allows for defect-free growth.

1.3 PERIODIC TEMPLATE

Another potential application of twist boundaries takes advantage of the periodic dislocation structure to produce a modulated surface topography. **Figure 11** provides a schematic of the concept. As was seen in **Figure 4** and **Figure 5**, there is a short range periodic stress field associated with the dislocations of a twist boundary. If one half of a twist-bonded bicrystal is made very thin, within the influence of this stress field, then

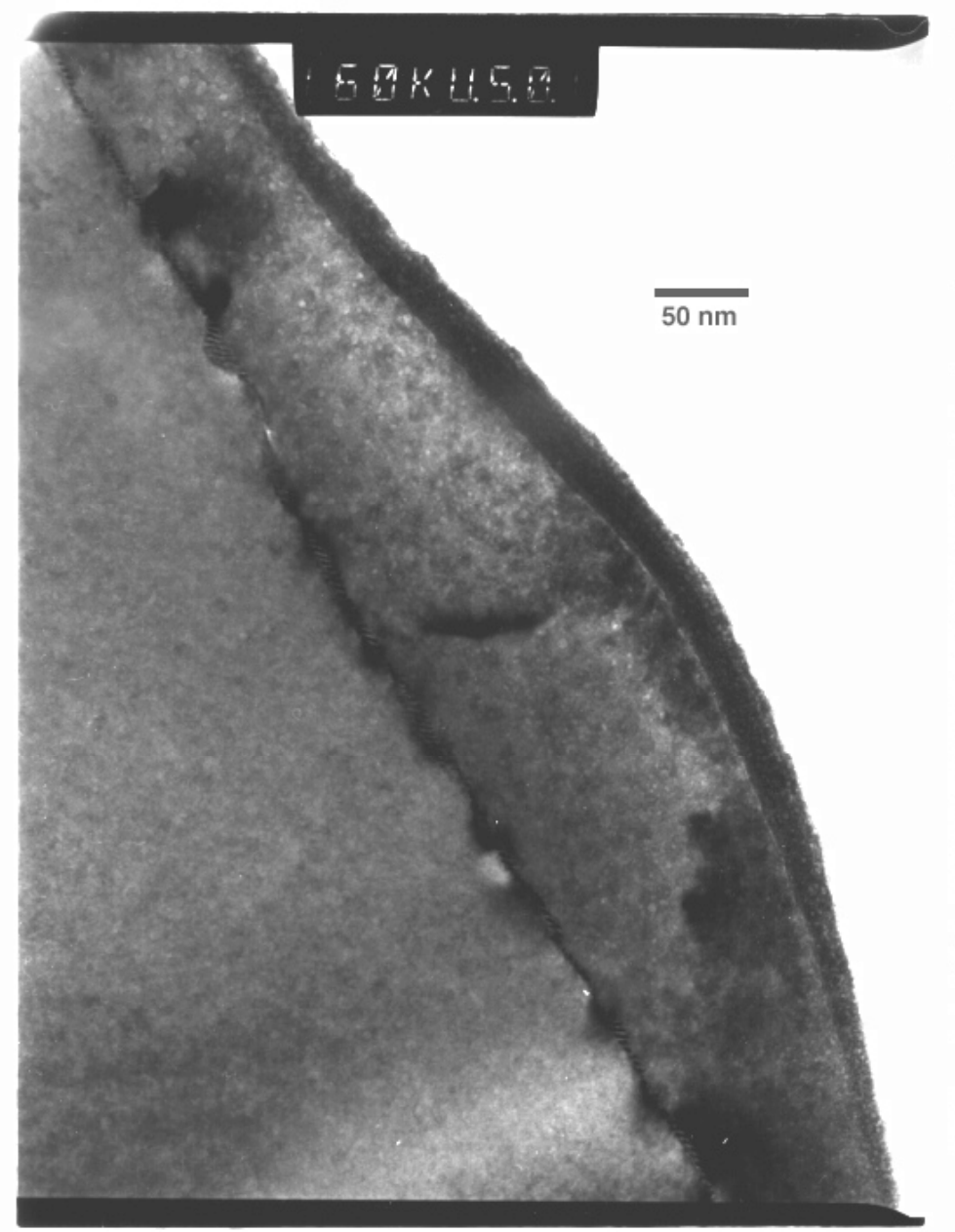

Figure 9: GaSb grown on GaAs using CUS process

(Micrograph courtesy of Dr. Shanthi Subramanian)

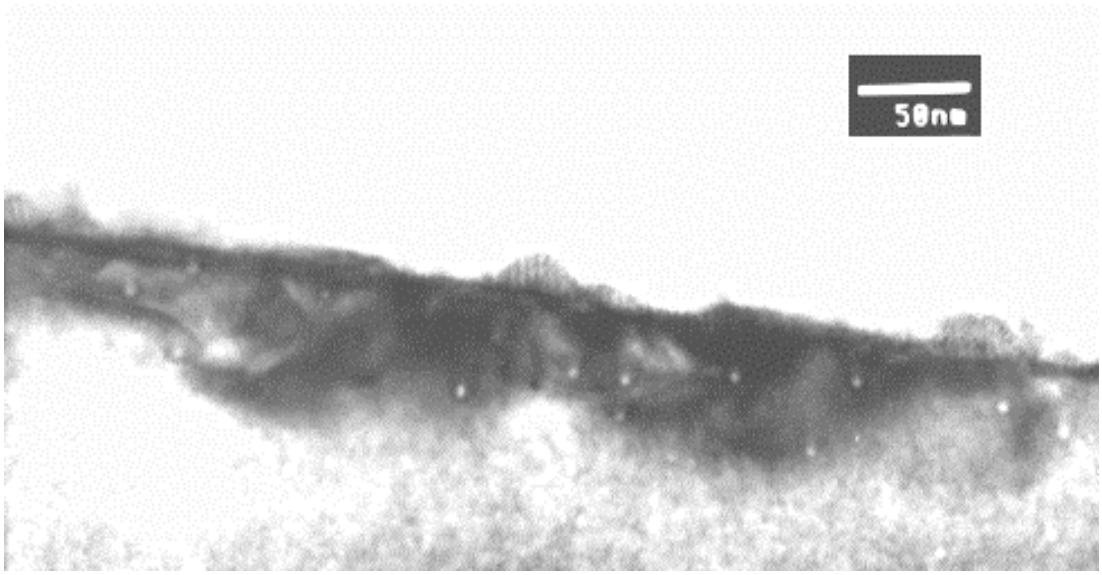

Figure 10: Interface region between GaSb and GaAs bicrystal containing the twist boundary (Micrograph courtesy of S. Subramanian)

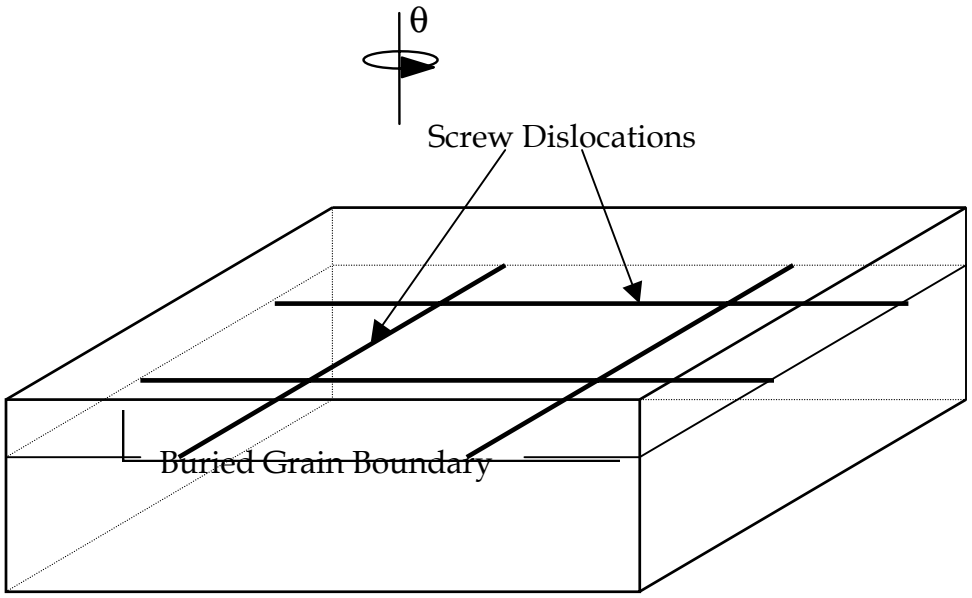

Dislocation Structure

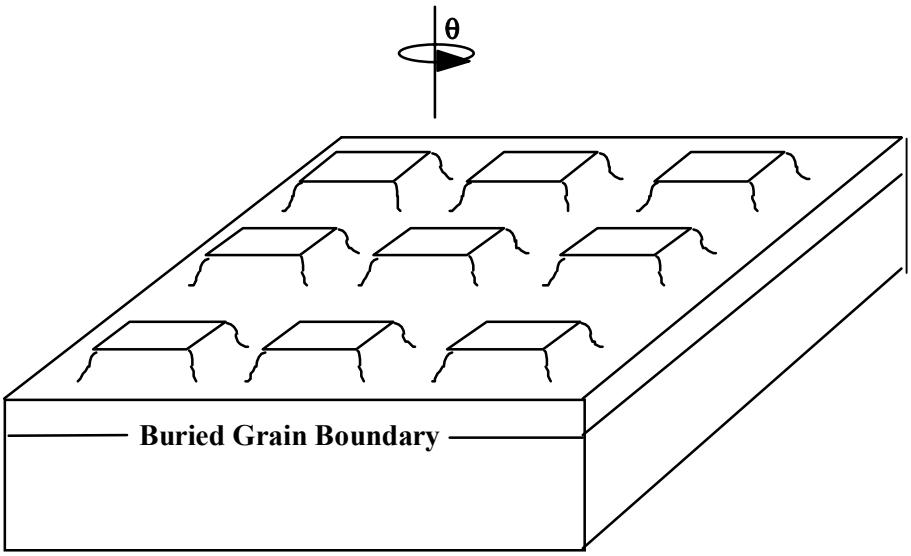

Topographical Structure

Figure 11: Schematic representation of the periodic template concept

the surface of the thinner half of the bicrystal may lower its energy by adopting a similarly periodic topography. Since such a relaxation would create excess surface area, the height of such 'hills and valleys' would be determined by some equilibrium between reduction of strain energy and creation of surface energy. The period of the structure would be determined by the spacing of the underlying dislocations. Dislocation spacings for low-angle twist boundaries range between 2 and 50 nm, as described by Frank's Rule. If such a surface could be created, this would provide control of topology at dimensions previously unachievable.

Applications for such a structure are many and varied. Due to the variations in height and curvature of the surface, growth of materials will occur differentially in the hills and in the valleys. An obvious potential application is for the creation of square arrays of quantum dots. A different, yet equally exciting possibility, is for the production of magnetic recording media. The information density of a recording media where the domains are 5 nm in size would be orders of magnitude greater than anything currently available. The regularity of their spacing would also provide advantages over other nano-scale magnetic materials, where the magnetic particles tend to be randomly dispersed throughout some inert media. Biological materials, such as proteins, have highly structure- sensitive growth behavior and a periodic template like the one proposed may provide interesting possibilities for the fabrication of biological materials.

There are several particularly appealing characteristics of this process. The most obvious of these is the scale of the structure. Spacings of 2 to 50 nm are not available with any current technique. Electron beam lithography can be used in the upper end of this range, but it is a serial process, i.e. it must

form each feature one at a time, line by line. The twist-bonded periodic template process forms arrays of features all in one process step. Another advantage is that the material of the template may be varied to meet the requirements of the final product. As long as relatively large, thin single crystals of a material can be formed, there is no *a priori* reason why this technique would not be applicable to that material.

CHAPTER TWO:
EXPERIMENTAL PROCEDURE

2.1 COMPLIANT SUBSTRATE

Figure 12 is a schematic representation of the twist wafer bonding geometry used for production of CUS materials.[27] Two conventional GaAs wafers are used. On one wafer, a moderately thin layer of some material that etches differently than GaAs is grown. On top of this layer, a thin section (3-20 nm) of GaAs is grown, either by MBE or MOCVD. This wafer and the other GaAs wafer, on which nothing has been grown, are cleaned. Organics are removed from the wafer surface by ultrasonic cleaning in acetone for one minute, followed by isopropyl alcohol for one minute, followed by deionized (DI) water for two minutes. The wafers are then dipped in a 10:1 HF solution in order to remove the native oxide layer. They are then placed together face-to-face such that the thin GaAs layer is in contact with the surface of the other wafer. The [100] axes of the two crystals are kept parallel and the two wafers are misoriented by a large angle, typically 40°, about this axis. This configuration is then subjected to heat and pressure, typically several MPa at ~560°C, in a reducing atmosphere so as to create an interfacial bond. Subsequently, both the GaAs substrate and the etch-stop layer are removed from the back of the thin layer, resulting in a thin, twisted layer bonded to a bulk GaAs substrate. This twist wafer bonding produces a large angle twist boundary at the interface. After removal of the etch stop layer, the CU substrate is ready for heteroepitaxial growth.

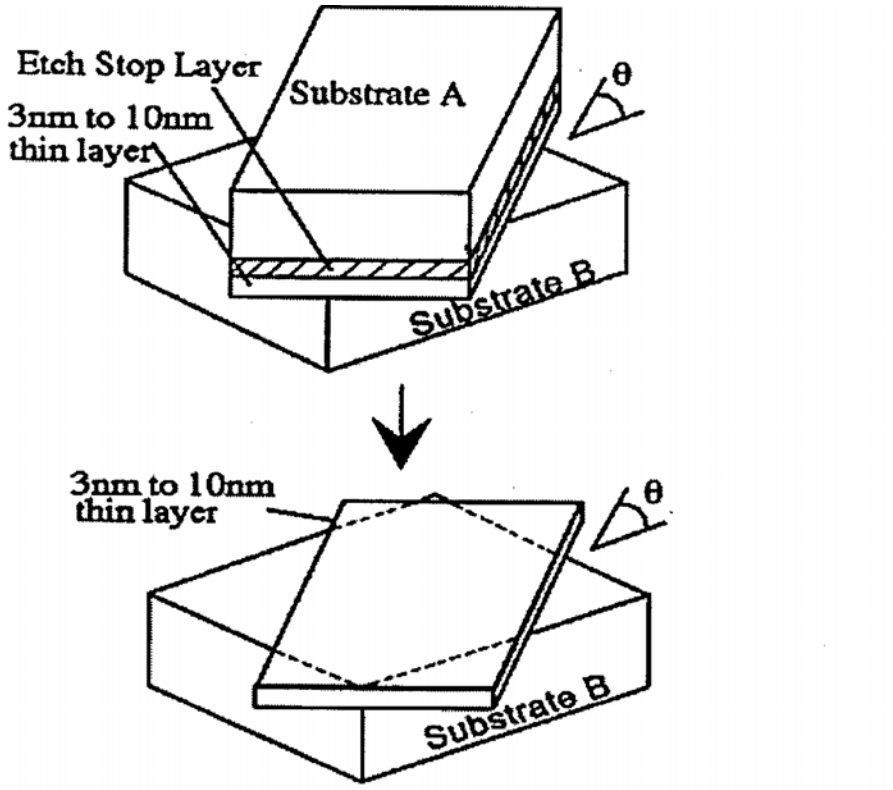

Figure 12: Schematic of CUS process

A similar process is utilized for producing Si compliant substrate materials. Here the starting materials are a standard Si wafer and a Silicon-On-Insulator (SOI) wafer. The SOI wafers used for this project are produced by SOITEC International. An SOI wafer consists of three layers: a thick (x00 μm) semi-insulating silicon layer, a thin (x00-x000A) insulating layer, and a thin (x00 A) doped silicon layer. SOITEC uses ion implantation techniques to produce a buried oxide as the insulating layer. For Si compliant substrates, the SOI wafer acts as the handle wafer and the thin oxide acts as the etch stop layer. Hot KOH is used to remove the handle wafer and buffered HF is used to remove the etch stop layer. Both etches are effectively infinitely selective. Particulars of the cleaning processes and bonding parameters for silicon wafer bonding will be discussed in a later section.

With respect to processing, the technique currently used by Professor Yu-Hwa Lo's group at Cornell University for wafer bonding is quite variable and produces only 1 small specimen for many hours work. Additionally, the success rate is not at the desired level. Most current wafer bonding techniques use differences in the coefficient of thermal expansion (CTE) in order to produce stresses at elevated temperature. The system used at Cornell for production of CU substrates uses aluminum chucks confined in a silica die to produce 1 cm^2 specimens.[27] Inhomogeneities and tight packing are both taken care of through the insertion of molybdenum foils. This introduces a great deal of variability in the pressures actually achieved, such that the pressure is neither predictable nor reproducible.

Previous research on GaAs wafer bonding has shown that the pressures required for successful bonding are between 1 and 3 MPa (~100 - 300 psi). Preliminary calculations show that the stress generated by the CTE

mismatches can be on the order of 100 MPa, one order of magnitude greater than what is required. Cracking of the wafers during bonding has provided macroscopic evidence of these exorbitantly high stresses. Additionally, using CTE mismatches limits the pressures that can be used by directly linking the pressure generated to the temperature applied. It was felt that a device for wafer bonding which allows for control of the applied pressure would be a step forward. A new design for the production of 1 in^2 specimens has been prepared with the John Sinnott of the Cornell MS&E Materials Preparation Facility. **Figure 13** shows the assembly drawing of this wafer bonding vise. The new design can be described as a spring loaded vise. The vise has three sets of jaws, one fixed and two free. Two rails run through the fixed and mobile jaws. Bellville washers, manufactured of Inconel 750 in order to withstand the high temperatures of the bonding process, are placed between the two free jaws. Compression of these washers provides the desired load. This design allows one to establish the applied pressure independently of the temperature. The jaws have been designed with removable inserts so that various geometries can be accommodated.

One CUS specimen was examined by the author. The specimen contained two films of Ge grown on Si, one with a compliant layer and the other without. Ge has a 4% compressive lattice mismatch with Si. All investigation was carried out on the JEOL 1200EX transmission electron

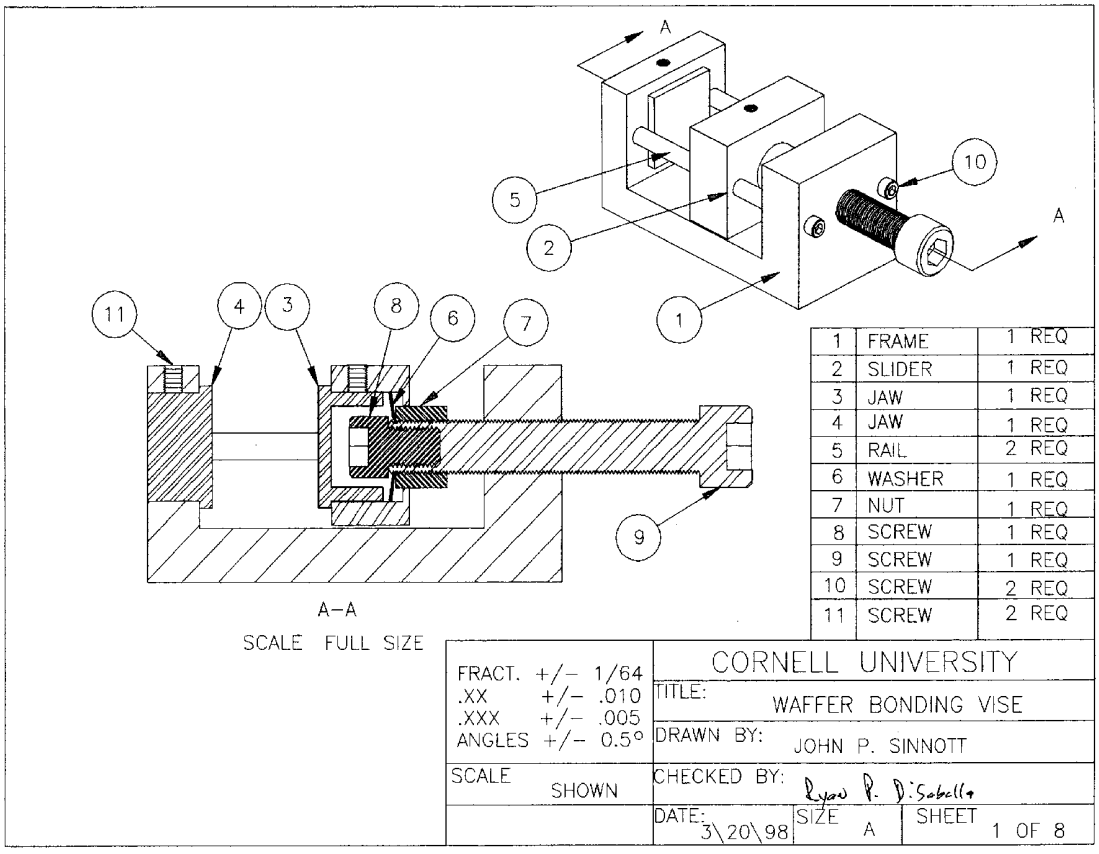

Figure 13: Assembly drawing of wafer bonding vise

microscope. The CUS materials were prepared by Rong Zhou and Yucai Zhou of Cornell University. The actual TEM specimen was prepared by Rong Zhou.

2.2 PERIODIC TEMPLATE

The periodic template project utilizes the same basic geometry for the fabrication of the twist boundary as the compliant substrate. In order for the stress field of the boundary to influence the surface of the bicrystal, one of the bonded crystals must be a few tens of nanometers thick, that is, $t \sim d_{dislocation}$. The angle of twist must be small in order to keep the dislocation spacing, and therefore, the allowable thickness of the second crystal, as large as possible. Research on the production of periodic templates was carried out using three material systems: GaAs, Si, and Au.

2.2.1 GaAs Periodic Template

The GaAs specimen used for investigation of the periodic template was originally produced as a bonding trial for the compliant universal substrate project. It was fabricated by Lakshmi Srivatsa and David Crouse of Professor Yu-Hwa Lo's group at Cornell. The specimen was received after bonding and after the handle wafer had been removed. As such, it consisted of a 500 μm GaAs wafer with a 3.2 nm thick twist bonded GaAs layer and a 50 nm thick InGaP etch stop layer. Srivatsa and Crouse attempted to form the bond with a 0° angle of twist.

Because of the inherent variability of the process and small local variations in single crystal orientation, this means that the actual misorientation angle was somewhere between -0.5° and +0.5°.

The InGaP etch stop layer was removed by etching in HCl. This acid will attack InGaP but should not etch GaAs at all. However, HCl can attack gallium oxide. Removal of the etch stop layer was checked via Rutherford Backscattering Spectroscopy using 0.9MeV He^{++} ions. In an attempt to allow surface topography to form, the specimens were annealed multiple times at 200°C for two hours in an H_2 atmosphere. The surfaces of the specimens were characterized with an Atomic Force Microscope (AFM).

2.2.2 Silicon Bonding

Before the relatively expensive SOI wafer was to be used, it was decided that reproducible procedures for bonding of plain silicon wafers should be determined. The wafers used were both n-type and p-type, grown by both Czochralski and Float-Zone Refining techniques. All wafers had [001] surface orientations. Typically, 1 in^2 pieces were cleaved from the wafers to test the various cleaning and bonding schemes.

All wafer cleaning was carried out in the Cornell Nanofabrication Facility (CNF). Two wafer cleaning techniques were attempted. The first technique removed organics from the wafer surface by ultrasonic cleaning in acetone for one minute, followed by isopropyl alcohol for one minute, followed by DI water for two minutes. The wafers were then dipped in a dilute HF solution in order to remove the native oxide layer and hydrogen terminate the surface. The two wafers were then clamped together face-to

face in an attempt to create a hydrogen bond across the surfaces. The HF dip and clamping were repeated until the wafers remained together.

The second wafer cleaning technique used a standard RCA clean to remove organics, metals, and particles from the surface of the wafers. The RCA cleaning procedure was developed by the RCA Corporation as a method to guarantee the removal of particulates and of such deleterious species as Na and Sn from the surface of wafers used in transistor fabrication. **Table 2.1** lists the solutions of the RCA cleaning procedure used, which is the standard MOS cleaning procedure used in the CNF.[29] The cleaned pieces were then subjected to same HF dip and clamping, as were the specimens cleaned via the first technique. Again, the hydrogen termination and clamping were repeated until an interfacial bond formed.

TABLE 2.1

RCA CLEANING PROCEDURE

Solution	Action
$NH_3OH:H_2O_2:H_2O$ (1:1:3)	Removes organics and particulates
$HCl:H_2O_2:H_2O$ (3:1:1)	Removes metals
$HF:H_20$ (1:6)	Removes native oxide, hydrogen terminates surface

Two different bonding processes were investigated. One process utilized the vacuum tube furnace of the Technical Operations Lab at Cornell University. The specimens were placed in a furnace which was subsequently pumped down until the vacuum was in the 10^{-7} torr range. The furnace temperature was increased at a rate of 10°C/min until the desired bonding temperature of 950°C was achieved. The specimens were then held at this soak temperature for one hour. Some specimens were loaded with a dead weight in an attempt to improve surface contact of the two wafers.

The other bonding technique used the Brew Press located in the Materials Preparation Facility of Cornell University. The Brew Press is a hot press equipped with graphite push rods and heating elements in order to withstand extreme temperatures and atmospheres. Specimens were heated to 1200°C for 68 hours. Load was supplied by a 3 kg Mo weight, which resulted in an approximately 3 MPa applied pressure. The chamber of the Brew Press was evacuated to the 10^{-4} torr range.

Transmission electron microscopy was attempted on all specimens. Very few specimens survived the preparation techniques required to produce TEM samples. Survival was considered to be the first measure that a bonding experiment was successful.

2.2.3 Gold Periodic Template

Due to the relative difficulty of bonding Si, experiments using gold were begun. Gold offers several technological advantages over Si for production of twist bonded bicrystals. The most obvious is the absence of a native oxide. A native oxide may interfere with the formation of a surface topography. The absence of the native oxide also relaxes the cleanliness

requirements present in processing and thereby increases yield. Additionally, the actual bonding procedure can be carried out in modest temperatures and requires no special atmosphere.

Production of a gold periodic template involved three distinct steps: production of one thick and one thin [001] oriented Au single crystal, bonding of these crystals, and selective removal of the substrate of the thin Au crystal. The Au single crystal films were produced via electron beam deposition and sputter deposition on [001] NaCl substrates.

Due to early difficulties with crystal quality, the thicker films used for the experiments detailed in this thesis were prepared several years ago by Dr. Michael Fitzsimmons for his synchotron diffraction study of FCC metal twist boundaries.[30] These films were grown via evaporation with a substrate temperature of 375°C and a vacuum of ~10^{-7} Torr.[31] In order to improve crystal quality, Dr. Fitzsimmons bombarded the NaCl substrate with electrons for ten minutes prior to deposition. The crystallinity and orientation of his thin film specimens were checked with backscattered Laue X-ray diffraction.

The thin films of Au were prepared by Gerhardt Schmidt of the Technical Operations Laboratory at Cornell University. Two techniques were used: electron beam evaporation and sputter deposition. Substrate temperatures of 200°C, 375°C, 450°C, and 500°C were all attempted. The 450°C substrate temperature was utilized by Phillip Lamarre for gold bicrystal fabrication in a study similar to that of Michael Fitzsimmons.[32] Additionally, specimens were annealed for 1 hour at 600°C after deposition. This post-deposition anneal was used by Keith Milkove in his dissertation research to reduce twin density in Au crystals.[33] Films greater than a few hundred Angstroms were characterized by backscatter Laue XRD while those thinner

than this were evaluated using the JEOL 1200 transmission electron microscope.

One thick and one thin Au crystal were bonded together in order to form the desired bicrystal. Bonding was carried out in the $MoSi_2$ hot press of the Materials Preparation Facility at Cornell University. The bonding was carried out with an applied pressure of ~1.0 MPa. The specimens were loaded and then the temperature was ramped at 3°C/min to 300°C. The specimens were held at this temperature and pressure for 1.2 hours. All processes were carried out in air. In order to facilitate later specimen preparation steps, the thin Au crystal is cleaved to be smaller in area than the thick Au crystal.

Specimens for the AFM must be quite flat. In order to achieve such flatness with our gold bicrystal we removed the NaCl substrate from one side only, the side of the thin Au crystal. The NaCl is left on the other side to act as a mechanical substrate. The NaCl specimen to be preserved is covered with nail polish (Wet 'n' Wild Midnight Blue). This is the motivation for making the thin crystal smaller in area: one can fully coat the lower substrate and cover some of its surface area to seal the edges. The specimen is then held in a beaker of water. To reduce the possibility of destroying the substrate crystal, only the crystal to be removed is submerged in the water.

The dislocation structure of the specimens was characterized with a JEOL 1200EX transmission electron microscope operating at 120kV. TEM specimens were prepared by flotation onto a copper grid. If the bicrystal specimen was not electron transparent, it was ion milled at 12° in a Gatan Duo-Mill. The surface of the thin half of the bicrystal was examined using a TechnoMetrix AFM equipped with Nanoscope II software.

CHAPTER THREE:
RESULTS AND DISCUSSION

3.1 COMPLIANT SUBSTRATE

No new CUS specimens have been prepared because of a lack of a research collaborator capable of growing heteroepitaxial films. The new wafer bonding device has recently arrived and preliminary GaAs bonding trials have begun. However, no conclusions have been drawn from this work as of this date.

Work has been carried out on the characterization of an older specimen, with Ge grown on Si. This represents a 4% lattice mismatch. A graphical solution of the Matthews-Blakeslee analysis shows that the maximum defect free thickness of Ge that can be grown on Si is 25 Å. **Figure 14** shows a bright field images of Ge films grown on Si. The film grown on the compliant layer is 100 nm thick, 40 times the Matthews-Blakeslee critical thickness. The presence of a domain structure in this film is immediately obvious. A closer inspection of the Si-Ge interface in these domains reveals that one set of domains exhibits contrast indicative of an interfacial layer while the other set of domains does not. **Figure 15 a, b** shows higher magnification bright field images of the interface in both types of domains. The presence of the interfacial layer in one domain and its absence in the other are apparent in these images. It was surmised that the interfacial layer was the compliant

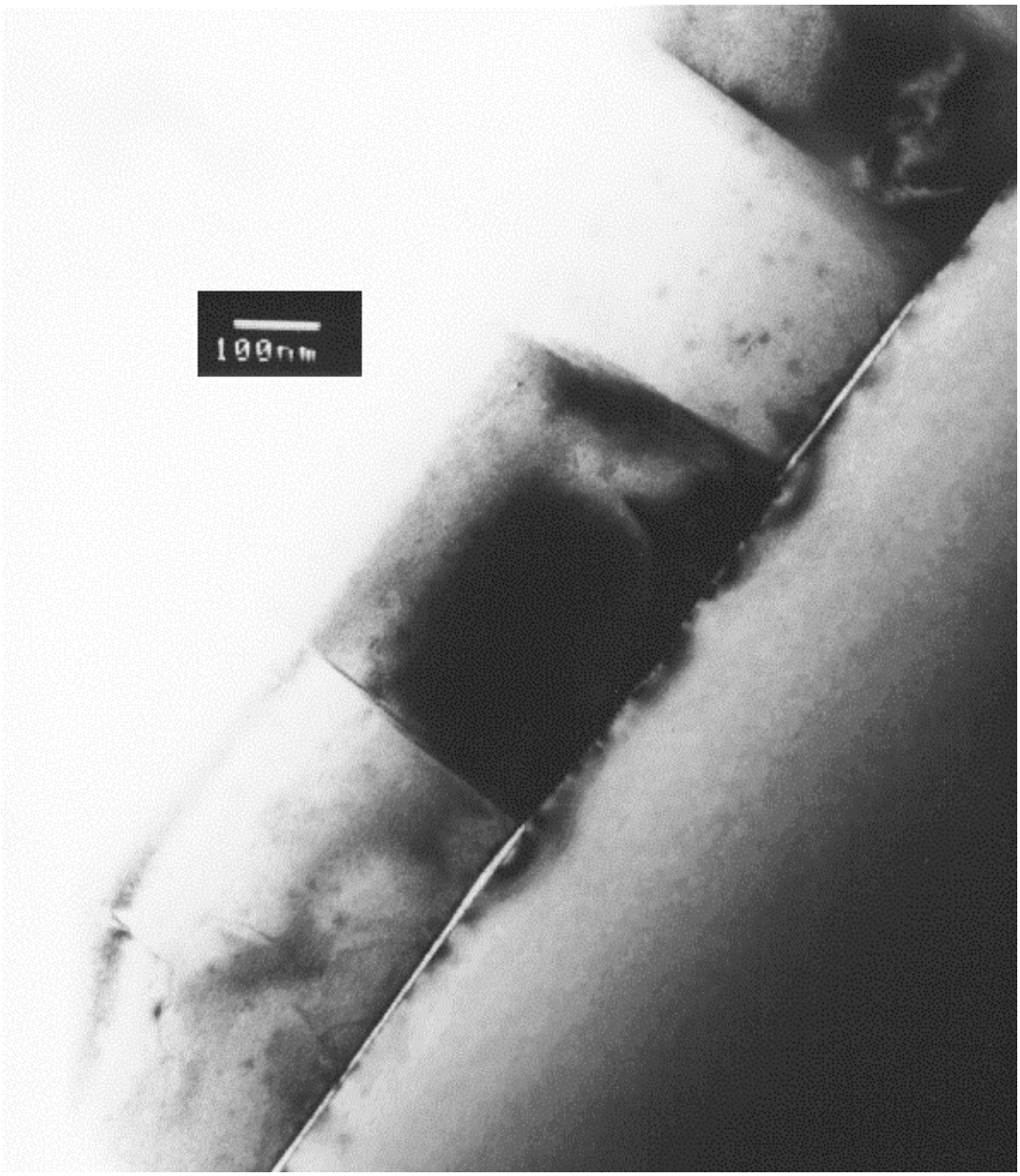

Figure 14: Bright field image of Ge grown on Si CU substrate

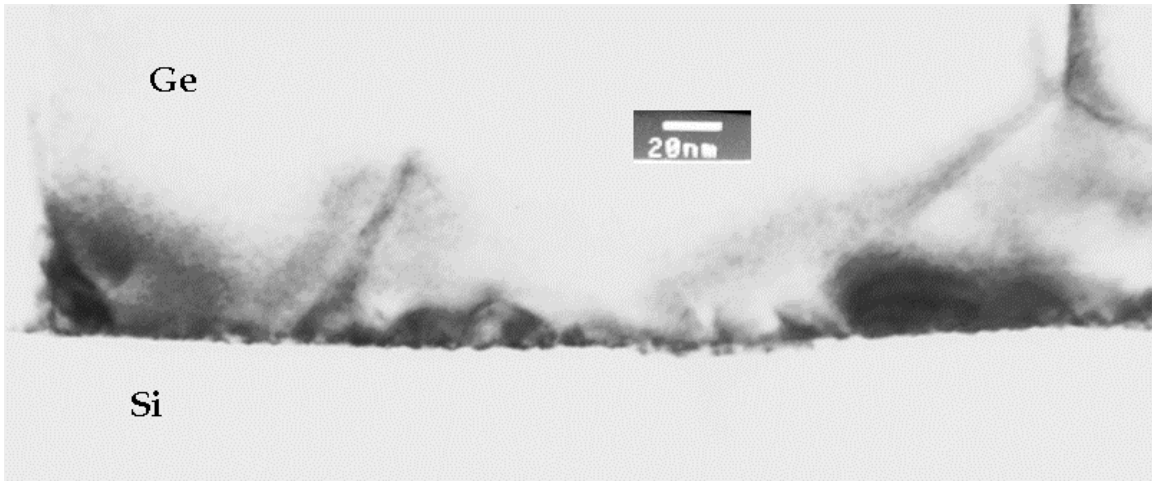

a) Interface in domain without compliant layer

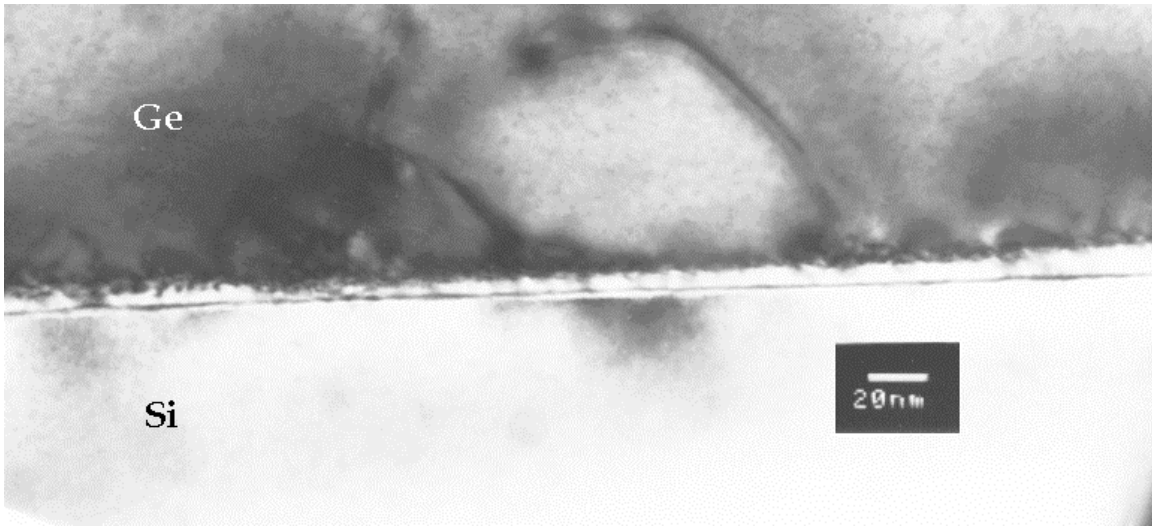

a) Interface in domain with compliant layer

Figure 15: Interfaces in both types of domains

layer and that it in the regions where it was not visible, the twist boundary had migrated out during the substrate heating that is carried out prior to epitaxial deposition. Evidence for similar twist boundary migration in gold has been observed by Allen and Goodhew.[34] Such a migration would lead to the formation of a tilt boundary between two neighboring Ge boundaries. **Figure 16** is a dark field, Ge and Si [400], image of a domain boundary containing a periodic contrast variation that is most likely a tilt boundary.

In order to validate the hypothesis that the domains represent the presence and absence of the compliant layer, SAD patterns were taken along both types of interface. The results are shown in **Figure 17 a, b**. In the SAD pattern of the region without the compliant layer, a rectangle of spots is visible near the transmitted beam. These spots were determined to be the [220] reflections of Si. In the specimen with the compliant layer, four spots exhibiting a four-fold symmetry are observable outside the rectangle of **Figure 17 a**. These are the [400] reflections of Ge. These results are consistent with the presence and absence of a compliant layer twist-bonded at a 45° misorientation angle.

High magnification bright field and dark field images were obtained of the interface in both types of domains in order to gain insight into what was happening at that interface. **Figure 18 a, b** shows the Ge [220] dark field images of the interfaces in two domains where the CU layer is not present. Localized contrast variations can be seen in the interface of the region of **Figure 18** a. This contrast variation is similar to the contrast that was seen at the GaSb/GaAs interface examined by Dr. Shanthi Subramanian, see **Figure 8.** Whether this interfacial 'puckering' is due to the migration of the twist boundary or to the stresses involved in heteroepitaxial growth

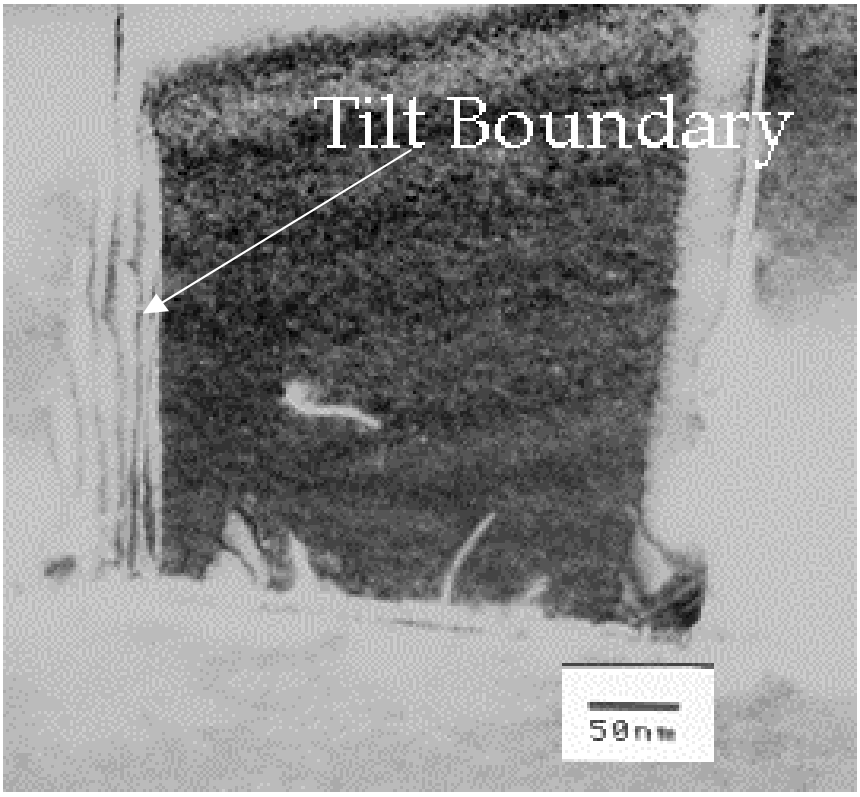

Figure 16: Dark field image of a potential tilt boundary between a twisted and untwisted region of the Ge film

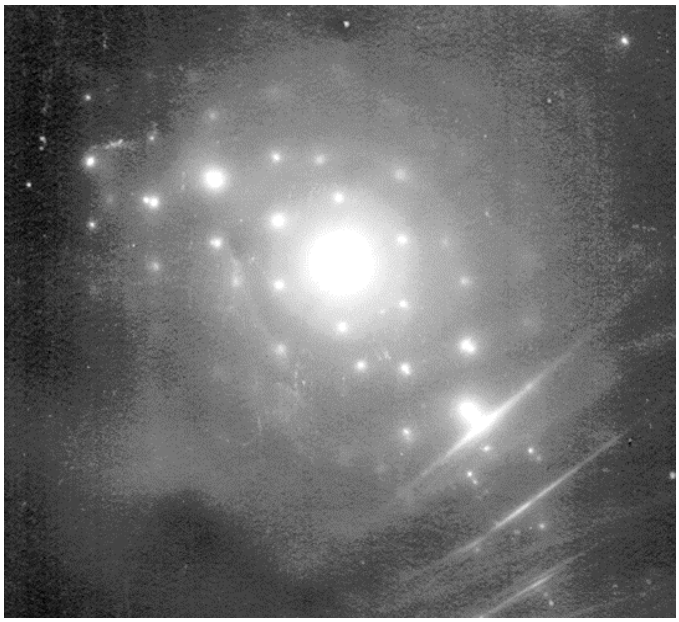

a). SAD pattern in region without compliant layer

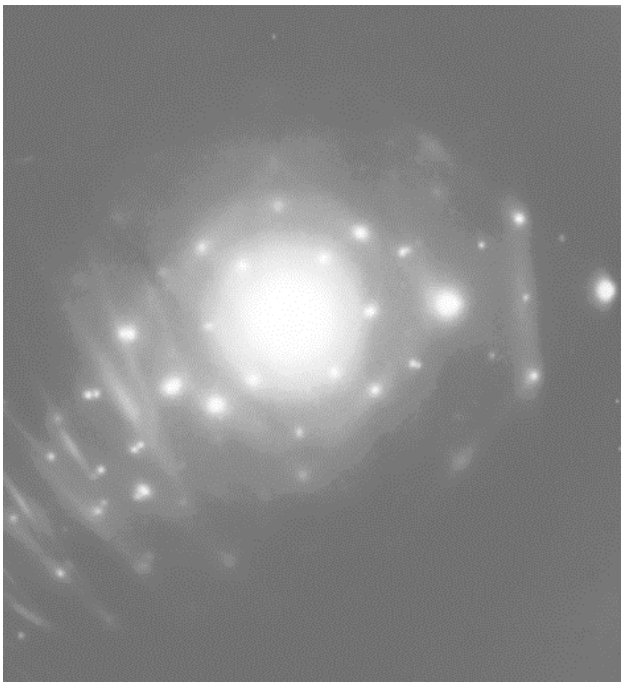

b). SAD pattern in region with compliant layer

Figure 17: SAD patterns from both types of domains

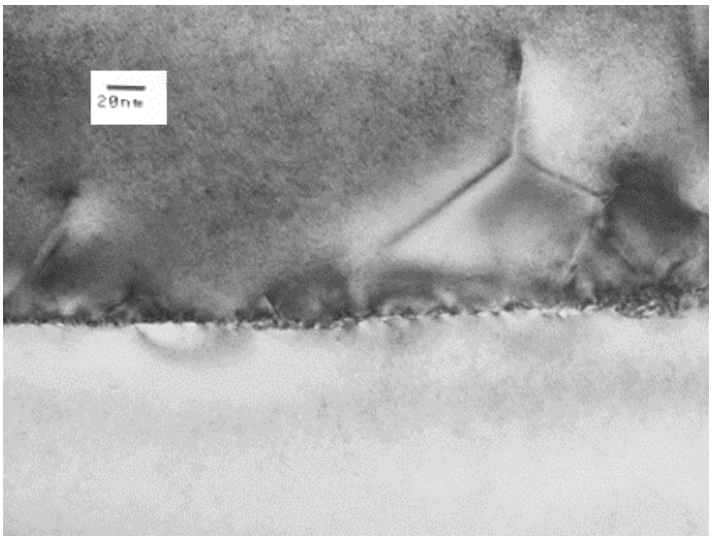

a). [220] dark field image of Si-Ge layer without CU layer

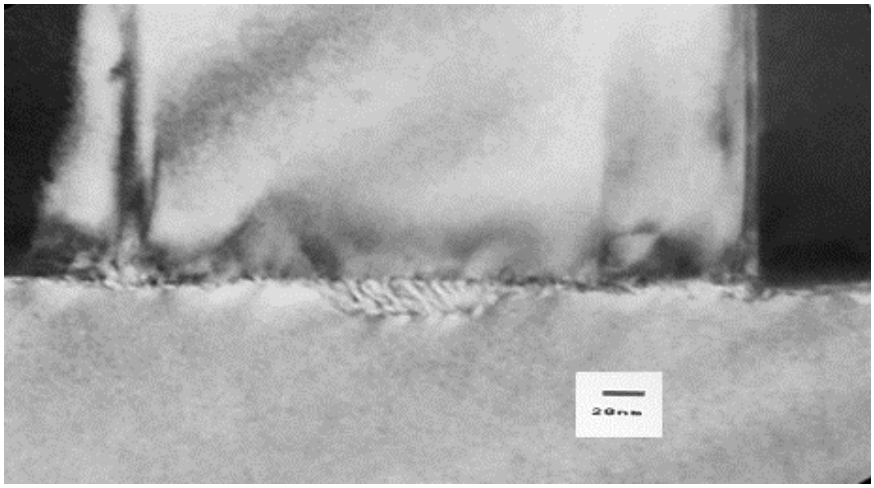

b). same diffraction condition as in a)., but a different region

Figure 18: [220] dark field images of Si-Ge interface without a compliant layer, taken in two separate domains

can not be determined at this point. A reasonably periodic contrast variation can be seen at the interface of **Figure 18 b**. This is probably caused by misfit dislocations at the interface. For a growth of pure Ge on Si, misfit dislocations would be found every 10 nm along the interface. The spacing of the contrast in this figure is slightly less than 10 nm.

Figure 19 is a bright field image of the interfacial region in a domain containing the compliant layer. Again, some interface structure is observable. The thickness of the compliant layer is ~4 nm. There are two additional regions of contrast associated with this layer. Below the complaint layer is a very thin, but very uniform, additional layer. This may be a thin oxide layer that formed during bonding. There is also a roughly periodic contrast variation on the top surface of the compliant layer. This contrast resembles that observed at the interface of the domain without a compliant layer. These variations may be due to misfit or other dislocations at this interface. This is a possible mechanism of the CUS. Misfit dislocations may form along the interface but may not be able to thread through the growth layer due to the pronounced stress field of the twist bonded layer.

Figure 20 shows a dark field image of the compliant layer produced with a [400] reflection of both silicon and germanium. The internal structure of the compliant layer is quite pronounced in this image. The thickness of the bright interfacial layer in this micrograph is ~5 nm, as opposed to 4 nm in the bright field image. It appears that, in this specimen orientation and diffraction condition, both the compliant layer and the layer immediately above it strongly diffract.

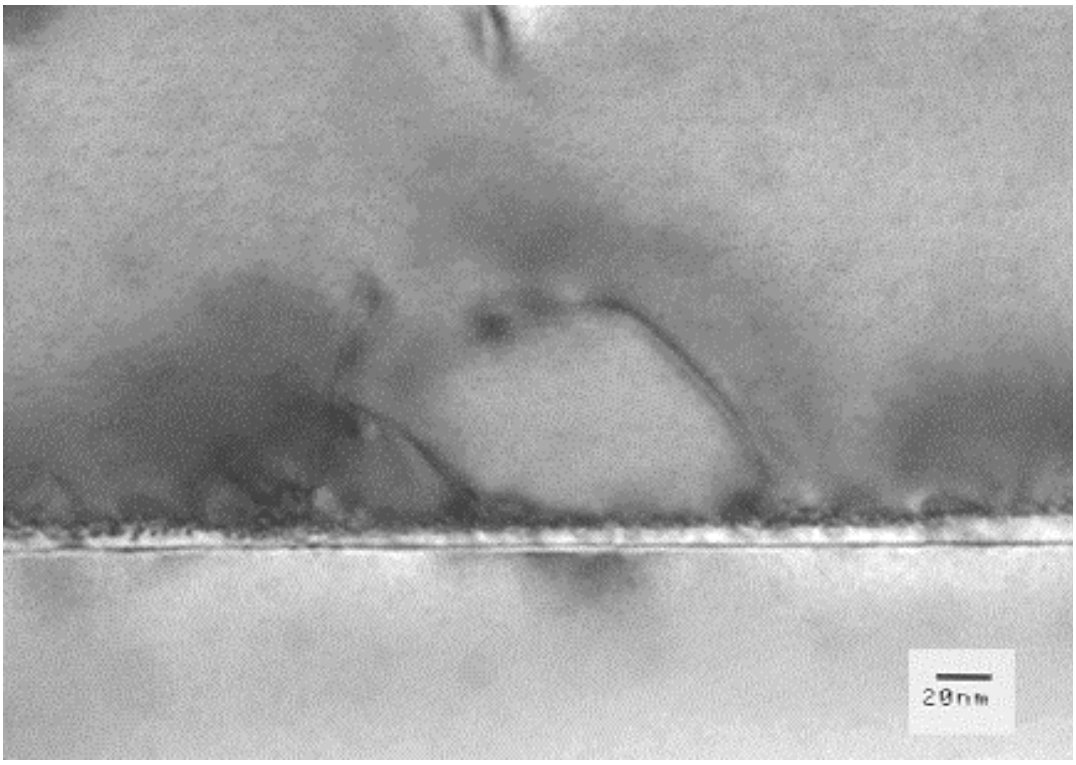

Figure 19: Bright field image of compliant layer at Si-Ge interface

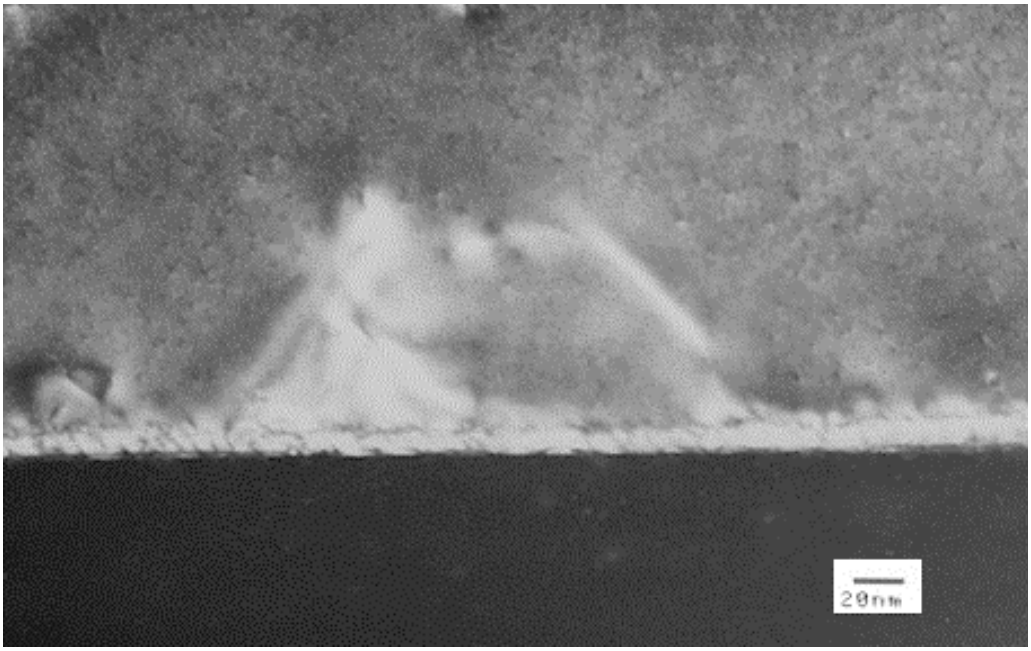

Figure 20: [400] Dark field image of compliant layer at Si-Ge interface

3.2 PERIODIC TEMPLATE

3.2.1 GaAs

Early results from the investigation of the GaAs specimens showed signs of having a periodic surface structure. **Figure 21** shows one of the early AFM scans of this surface. One can see a roughly periodic array of hills and valleys in this image. **Figure 22** shows a large area scan of the same surface. The rough, 'Rocky Mountain', topography of the surface cast doubt onto whether the periodic area seen in **Figure 21** was truly a result of the buried grain boundary or if it was a coincidentally approximately periodic surface. An RBS examination of the specimen showed the presence of Indium and Phosphorous on the surface. This showed that the etch stop was not completely removed and that the periodic structure of **Figure 21** was likely a fortuitous occurrence.

The specimens were then subjected to a series of HCl etches and anneals at 200°C in H_2 in an attempt to remove the remaining InGaP and allow the surface to relax. After the second such treatment the surface stabilized into the structure shown in **Figure 23**. Small area scans between the ridges shown in this figure revealed an essentially flat surface.

There are two possible explanations of such a surface. Srivatsa and Crouse have determined that this particular specimen contained a

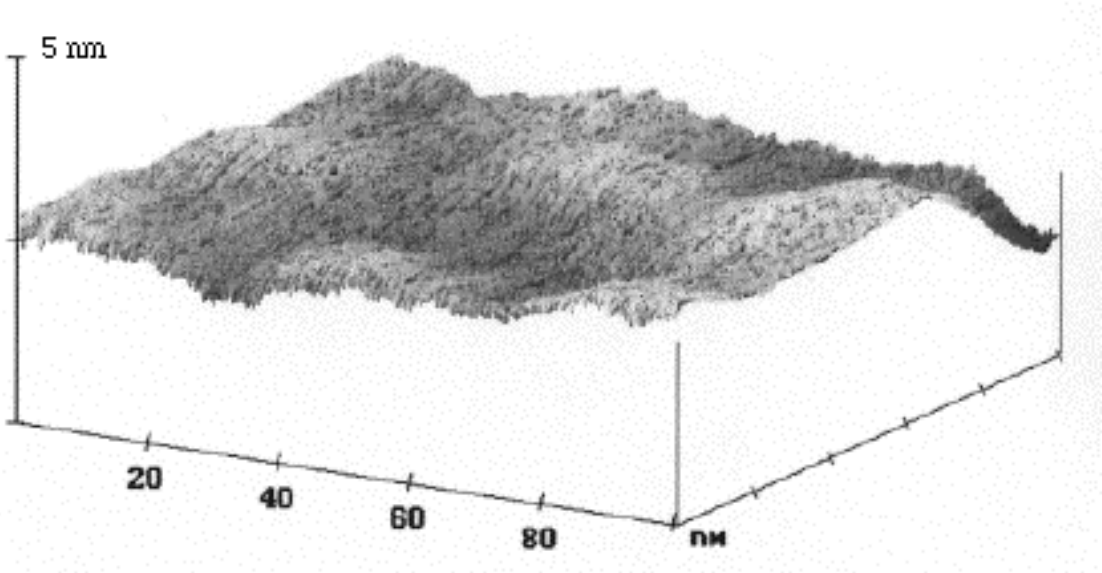

Figure 21: AFM scan of GaAs bicrystal

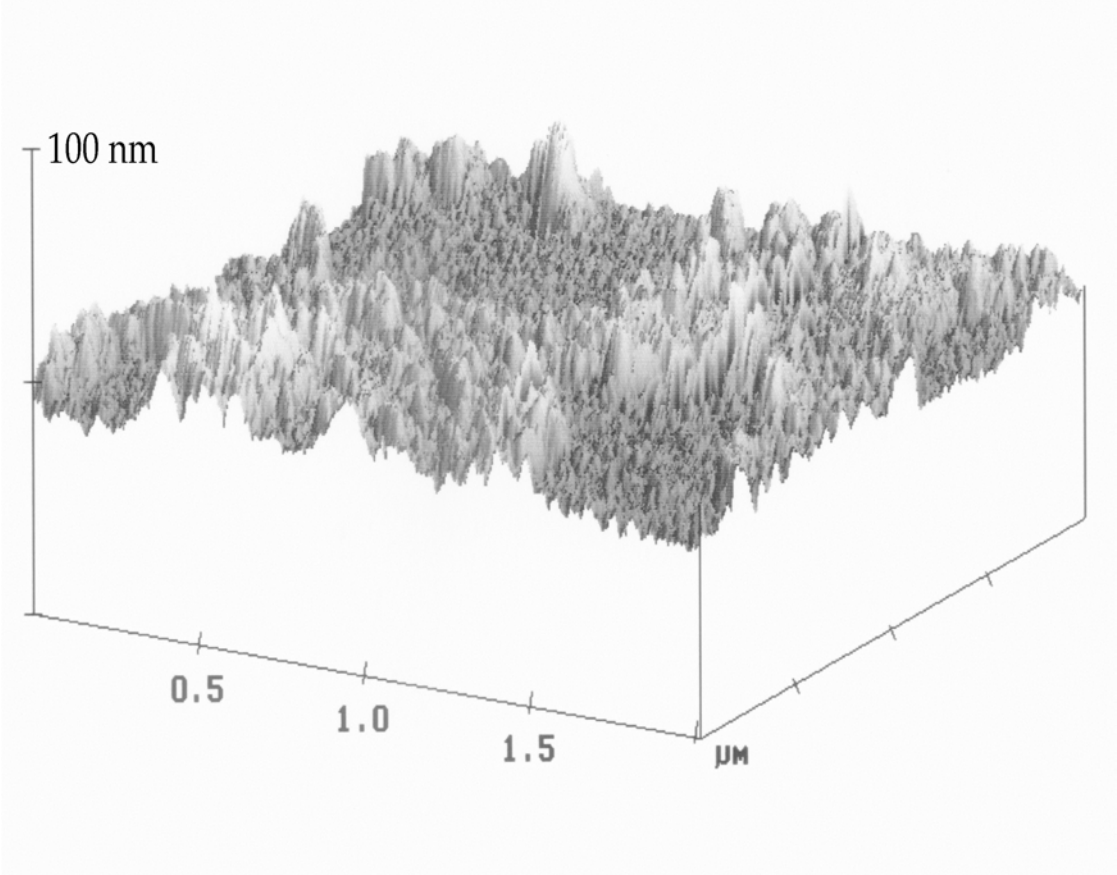

Figure 22: Large area AFM scan of GaAs bicrystal

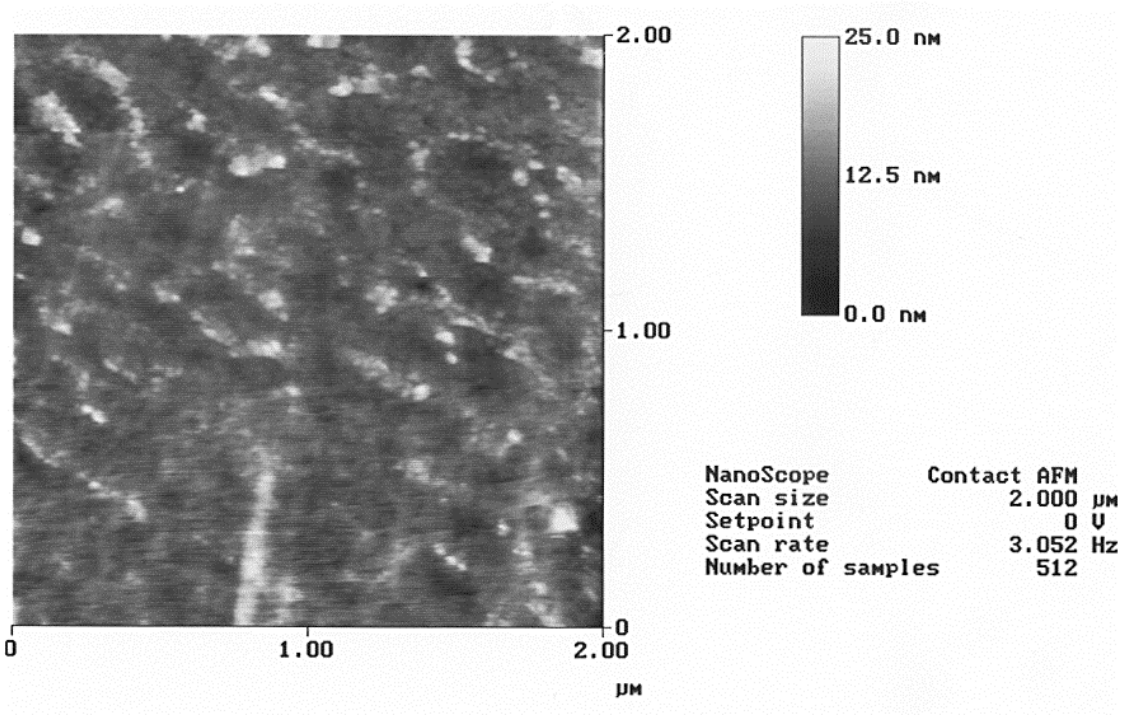

Figure 23: GaAs surface after etching and annealing

high defect density.[35] Additionally there have been difficulties with the quality of InGaP etch stop layers. Pinholes through the etch stop layer may have allowed the 4 nm twist bonded GaAs layer to be removed during the etching away of the handle wafer. The twist bonded layer may have also been removed during the repeated HCl etches. Although HCl does not attack GaAs it does attack its native oxide. Alternately, there may have been chemical defects in the InGaP layer that inhibited complete removal of the layer. A TEM specimen of the material was being prepared in order to determine if a twist boundary was still present. However, the specimen was destroyed during processing, so no definitive conclusions can be drawn.

These difficulties illustrate one of the potential problems in producing a periodic template from materials that form a native oxide. In order to allow the strain field of the boundary dislocation structure to influence the bicrystal surface, one of the crystals must be very thin, no more than a few hundred Angstroms thick. Native oxides tend to be several tens of Angstroms thick; a number which, under these conditions, is a significant fraction of the crystal thickness. This oxide may suppress the surface relaxation such that a periodic surface topography is not formed. However, removal of the native oxide will consume a large fraction of the twist-bonded layer and can not be done repeatedly. A template structure that exists only in situations of low oxygen activity would have few useful applications.

For materials that form native oxides a slightly different process path may be most useful in producing a valuable product. As was mentioned in the Introduction, grain boundaries serve as impurity gettering sites. In oxide forming materials, one could dope the upper crystal with some material that etches differentially than the bicrystal material. Thus, the doped grain boundary dislocations could serve as a mask during an etching procedure. For example, in a silicon twist boundary, one could dope the dislocations with oxygen then dip the specimen in hot KOH. The resultant structure should be a surface with a square array of several nanometer high lines.

3.2.2 Silicon Bonding

The first silicon bonding attempts used Czochralski wafers, ultrasonic cleaning, and bonding in the MSC Technical Operations Laboratory (TOL) vacuum furnace. None of these trials were successful. Most specimens fell apart at the interface while in the vacuum furnace. Most of those that

survived came apart at the interface during TEM specimen preparation. Failure at the interface shows that either a weak bond was formed or that bonding occurred in only small areas of contact between the two wafers. An electron diffraction pattern of the one specimen that survived specimen preparation is shown in **Figure 24**. The amorphous rings are indicative of formation of an oxide. An interfacial oxide forms in lieu of a twist boundary and, for this project, must be avoided. This result, coupled with the work by Goessele *et. al.* on formation of oxides during silicon wafer bonding, lead to the abandonment of Czochralski grown wafers for bonding experiments.[7]

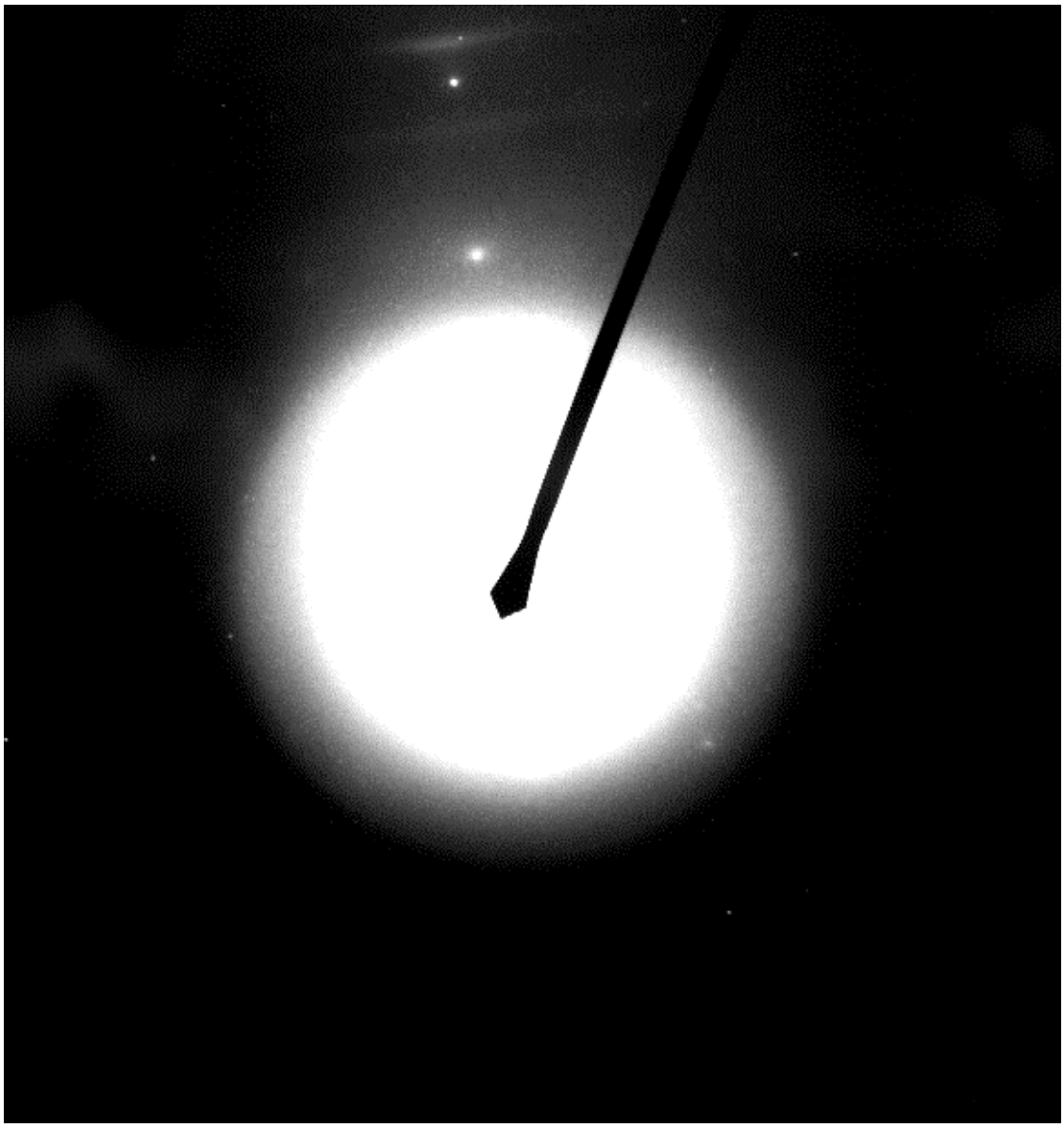

Figure 24: Electron diffraction pattern of twist-bonded silicon bicrystal

Trials were subsequently begun using Float Zone Refined wafers and an RCA cleaning process. Float Zone wafers are melted and recrystallized several times in order to reduce impurity concentrations. SiO_2 is the most common crucible used in the Czochralski method of silicon boule production and the oxygen content of such materials is quite high. The drastically reduced oxygen concentration of Float Zone Refined wafers greatly reduces the chances of forming an interfacial oxide layer. The RCA clean process is used commercially for the production of MOSFET devices and is known to produce exceedingly clean surfaces. Specimens processed in this manner were also bonded in the TOL vacuum furnace. More than half of these specimens survived the furnace treatment and possessed some sort of interfacial bond. Unfortunately, none survived cross-section TEM specimen preparation. However, none of these specimens failed along the interface; they fractured through the cross section of the silicon wafer. One specimen did not fracture at all, a hole was punched through it with a pair of tweezers. All of this is indicative of a strong interfacial bond.

One specimen was prepared using the Brew Press. This was prepared from two pieces of a Float Zone wafer. These pieces were given the ultrasonic clean and HF dip then placed into the graphite die of the Brew Press. This specimen held together through bonding and a cross section TEM specimen was prepared. This broke apart at the glue lines, again indicative of a strongly bonded interface.

These difficulties again serve to illustrate the point made in the previous section: production of a periodic template on a material that forms a native oxide will not be trivial. The presence of a nearby reservoir of oxygen may make formation of twist boundaries with SOI wafers exceedingly

difficult. Provided that this can be done, the question of whether or not a native oxide will allow surface topography to form still needs to be answered. However, with Si it may be possible to dope the boundary in order to preserve it for use as a lithographic mask, thus enhancing any dislocation induced surface topography.

3.2.3 Gold Periodic Template

The first step in the fabrication of a gold periodic template is the production of gold single crystals. Relevant process variables include substrate material and temperature, atmosphere in the deposition chamber, and deposition rate. All films were deposited on NaCl [001] substrates which were cleaved from irradiated NaCl rods immediately prior to placement in the deposition system. **Figure 25 (a, b)** shows a bright field image and a selected area diffraction (SAD) pattern, respectively, from a film sputter deposited at a substrate temperature of 200°C. **Figure 26 (a, b)** shows a bright field image and a selected area diffraction pattern, respectively, from a film sputter deposited at a substrate temperature of 375°C and then subsequently annealed for one hour at 600°C. The polycrystallinity of all these films is obvious in both the image and diffraction pattern. **Figure 27** shows the SAD pattern for a film electron beam deposited at 500°C. This diffraction pattern shows that this film was also polycrystalline. As is evidenced by the peaks in the diffraction rings, here is a strong [001] texture in all of the films, particularly the film of **Figure 26** which was given the subsequent annealing treatment.

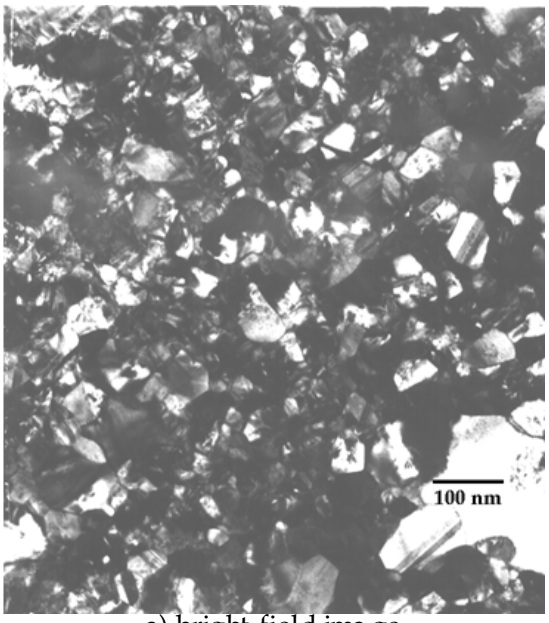

a) bright field image

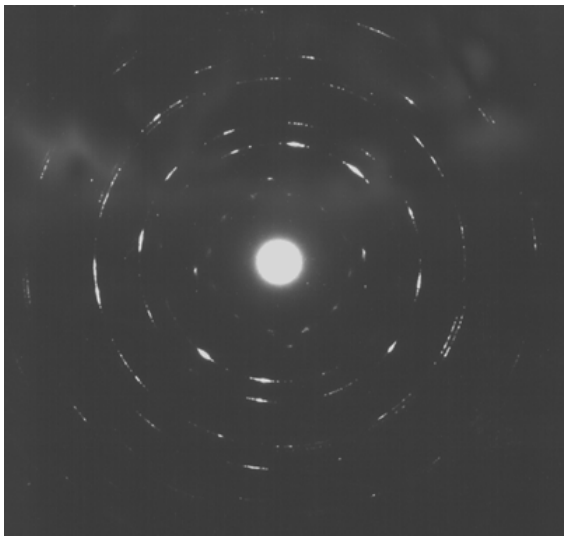

b) SAD pattern

Figure 25: Gold film, sputtered at 200°C

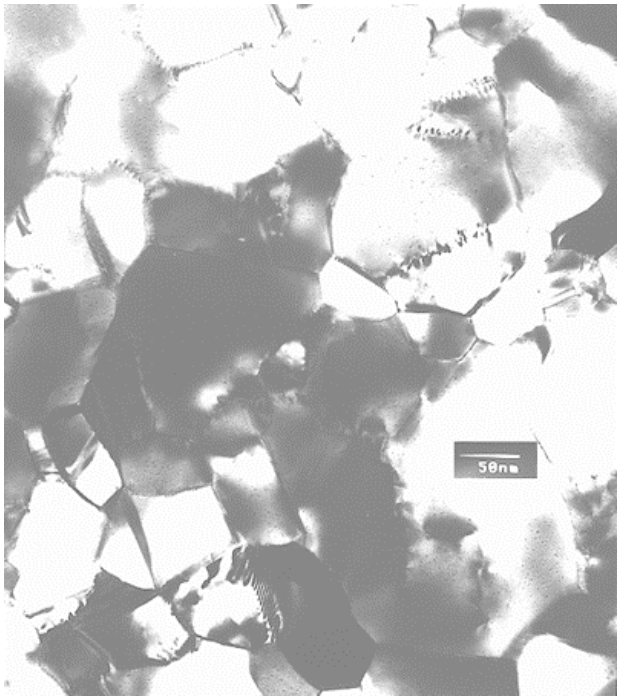

a) Bright field image

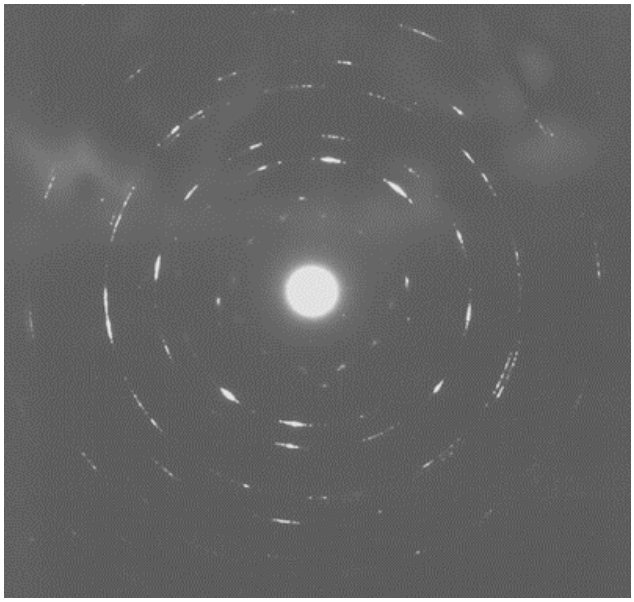

b) SAD pattern

Figure 26: Gold film, sputtered at 375°C then annealed for one hour at 600°C

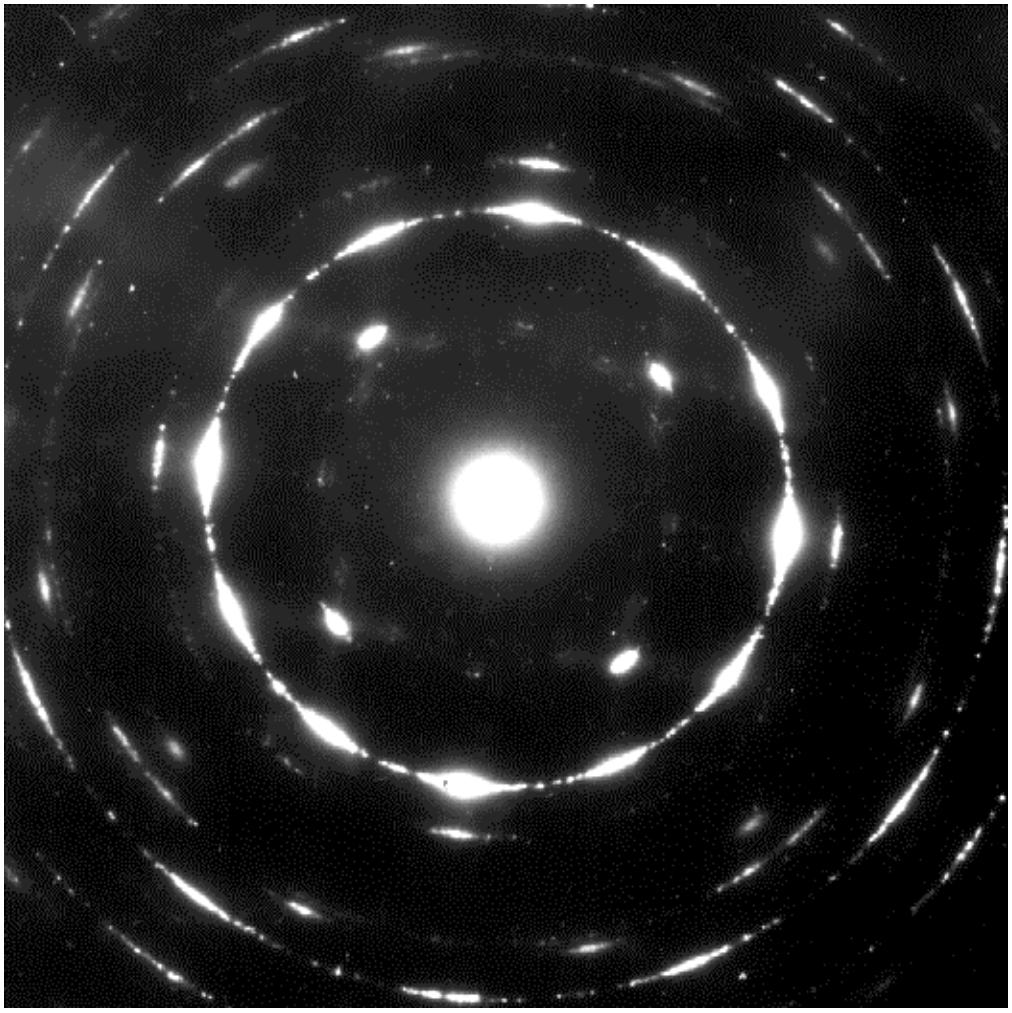

Figure 27: SAD pattern of film electron beam deposited at 500°C

Figure 28 shows the film that was sputter deposited at a 450°C substrate temperature. This film was also annealed at 600°C after deposition in order to reduce defect densities. One can see that it is a highly twinned single crystal. This specimen, which was approximately 20 nm thick, was used for twist bonding.

As was stated in Chapter 2, early difficulties in fabrication of single crystals lead to the use of previously prepared Au specimens. **Figure 29** shows the Laue patterns of a 5000Å Au film and a [001] NaCl slice. The only noticeable difference between the two patterns is the greater breadth of the spots in the Au containing pattern. As would be expected in a lattice matched, epitaxial growth, all peak positions are equivalent. The added breadth of the gold peaks is due to the higher defect density, i.e., twins and dislocations, of the gold compared to NaCl

The gold film of **Figure 28** was twist bonded to the film represented by the SAD pattern of **Figure 29** according to the procedure described in Section 2.2.3. A bond was successfully formed and the salt crystal that was the substrate of the thin gold layer was removed by dissolution in water. **Figure 30 (a, b)** shows the SAD pattern and bright field image of the resultant grain boundary. The square array of dislocations is immediately obvious. The dislocation spacing is 4.9 nm, which is consistent with the misorientation angle of 3.5° measured from the SAD pattern. The large dark bands are twin boundaries in one of the crystals. The regions where a single row of tightly

Figure 28: Film sputtered at 450°C

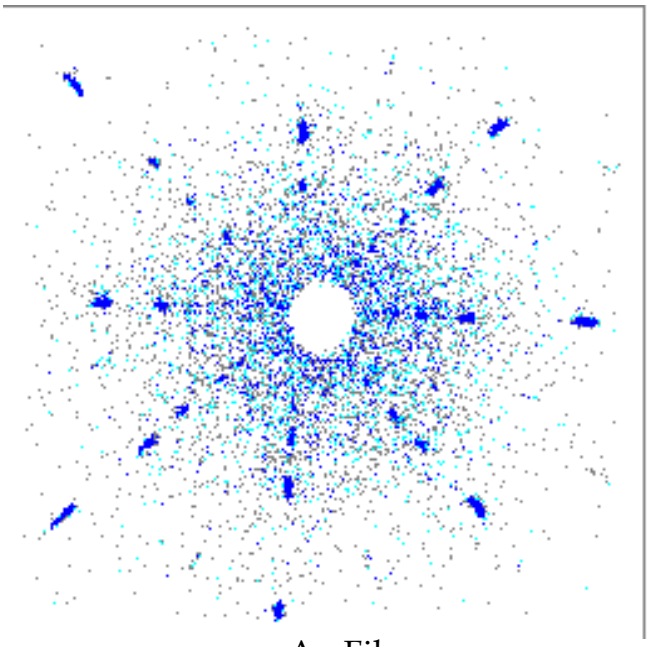

Au Film

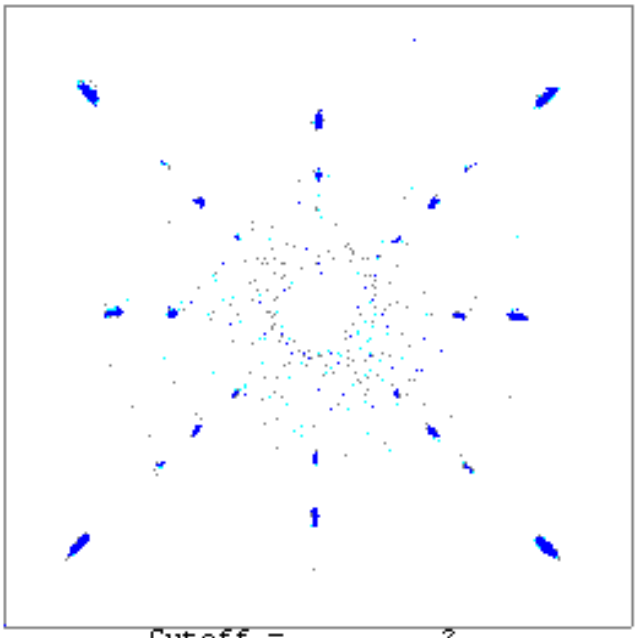

NaCl substrate

Figure 29: Backscatter Laue pattern of 500 nm Au film and NaCl substrate

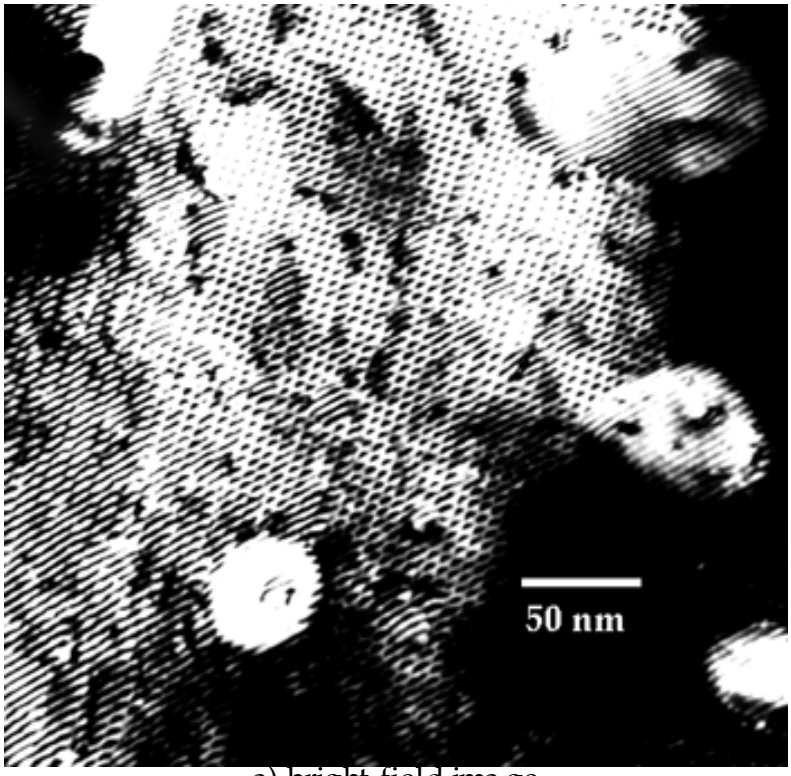

a) bright field image

b) SAD pattern

Figure 30: Au bicrystal, 3.5° misorientation

spaced fringes are visible are likely where the two crystals did not form a bond. These are Moiré fringes due to the two misoriented lattices in the path of the electron beam.

A large area AFM scan of the surface of this bicrystal is presented in **Figure 31**. The majority of the surface is flat, however, note the ridges on the upper portion of the image. In order to enhance any surface topography, after this image was taken one quarter of the specimen was cleaved off and annealed at 200°C for one hour in air.

Large area AFM scans were taken of the annealed specimen and the surface is relatively flat on a 10 nm scale. A smaller area was than examined with the AFM. The results of these scans are shown in **Figure 32 (a, b)**. The image on the bottom is from a scan rotated 30° from that of the upper image. The periodic hill and valley structure of the image is evident. Spacing of the peaks is 4.9 nm, which is nearly identically matched with the observed dislocation spacing shown in **Figure 31**. **Figure 33** compares the bright field TEM image of the dislocation structure and the AFM image of the surface, at the same magnification. Again, the parallelism between the two periodicities is apparent. **Figure 34** shows a scan, using the same microscope parameters, taken at a later time in another region of the specimen. The same hill and valley structure as was observed before remains evident. The AFM measured value of R_a for this surface was 2.4Å, suggesting an overall amplitude of the structure to be 4.8Å from peak to valley. The parameter R_a is the arithmetic mean deviation of surface height from its centerline.

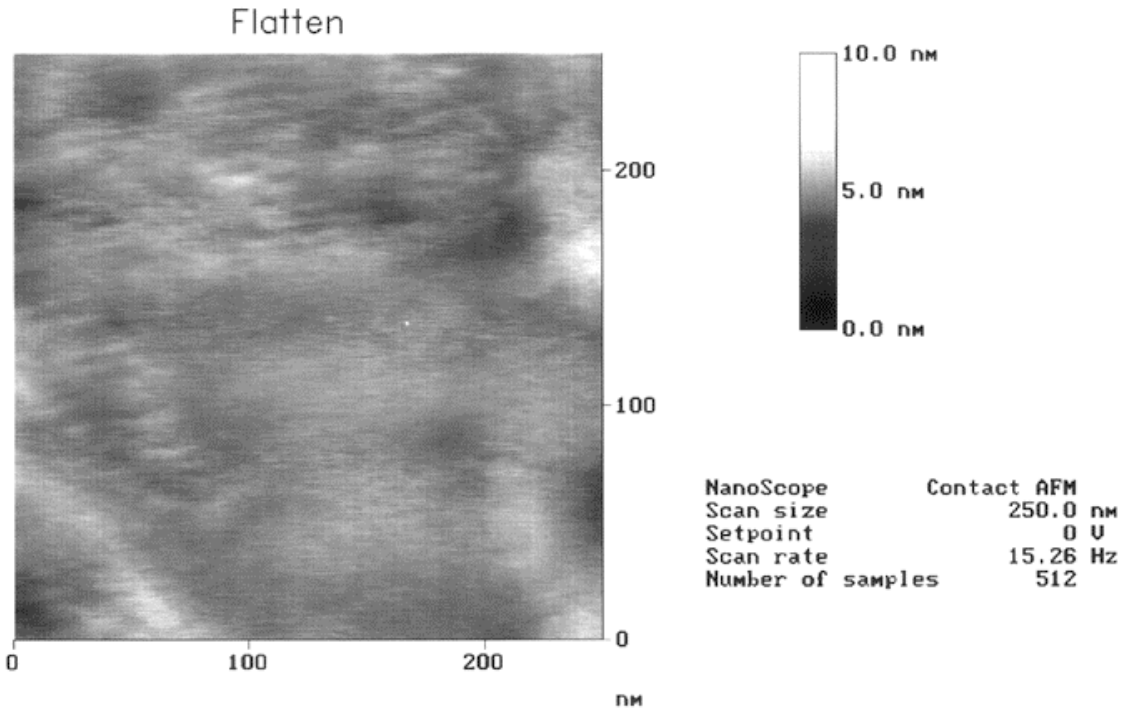

Figure 31: Large area AFM scan of bicrystal of Figure 30, as produced

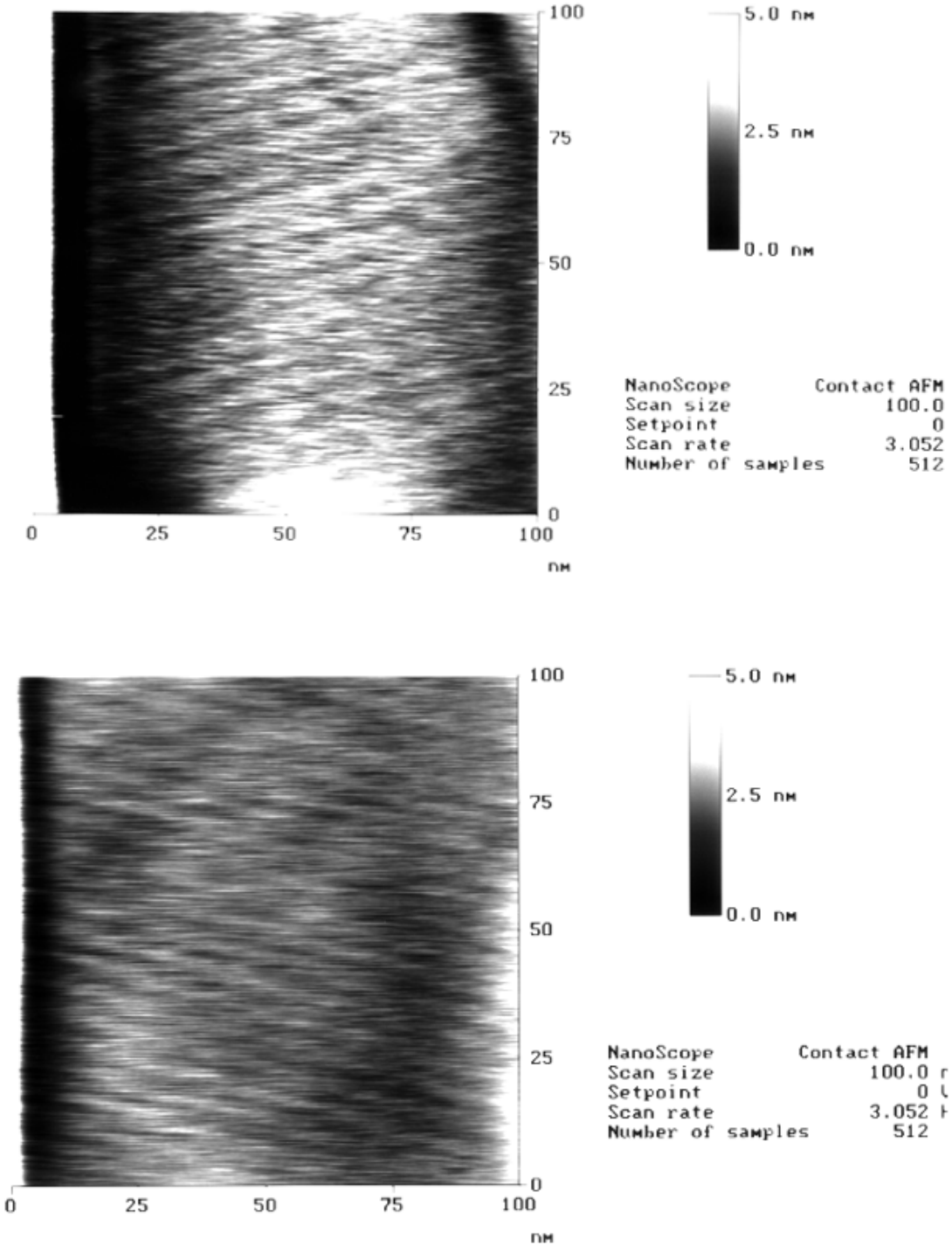

Figure 32: Small area scans of specimen from Figure 31, following anneal. Lower image is from scan taken 30° from that of upper image

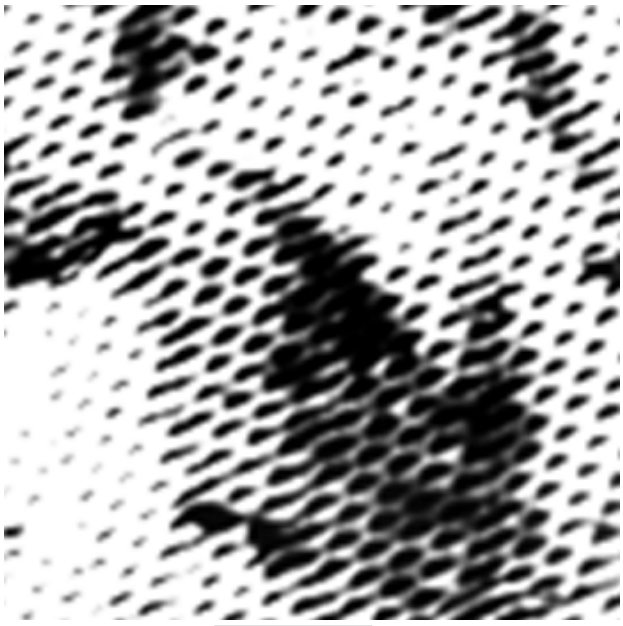

Bright Field Image

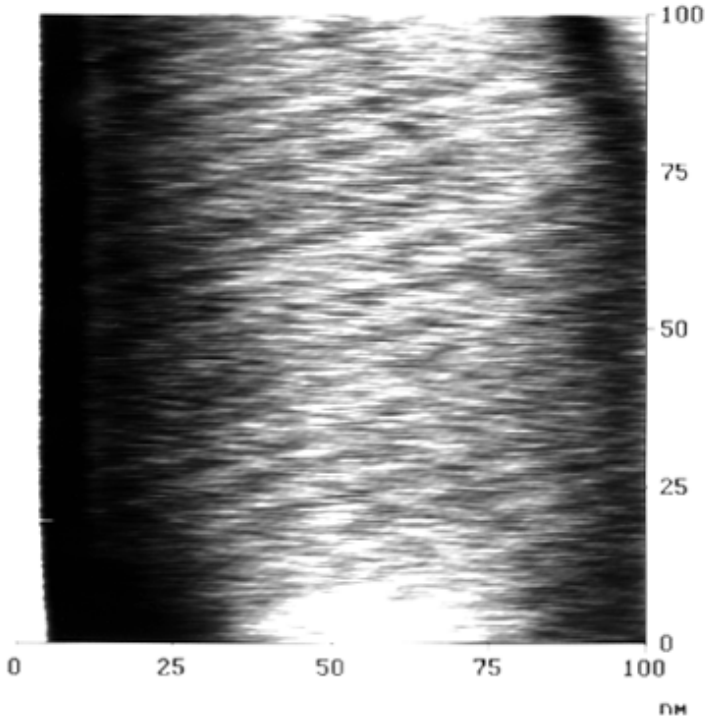

AFM scan

Figure 33: TEM and AFM images of 3.5° Au bicrystal

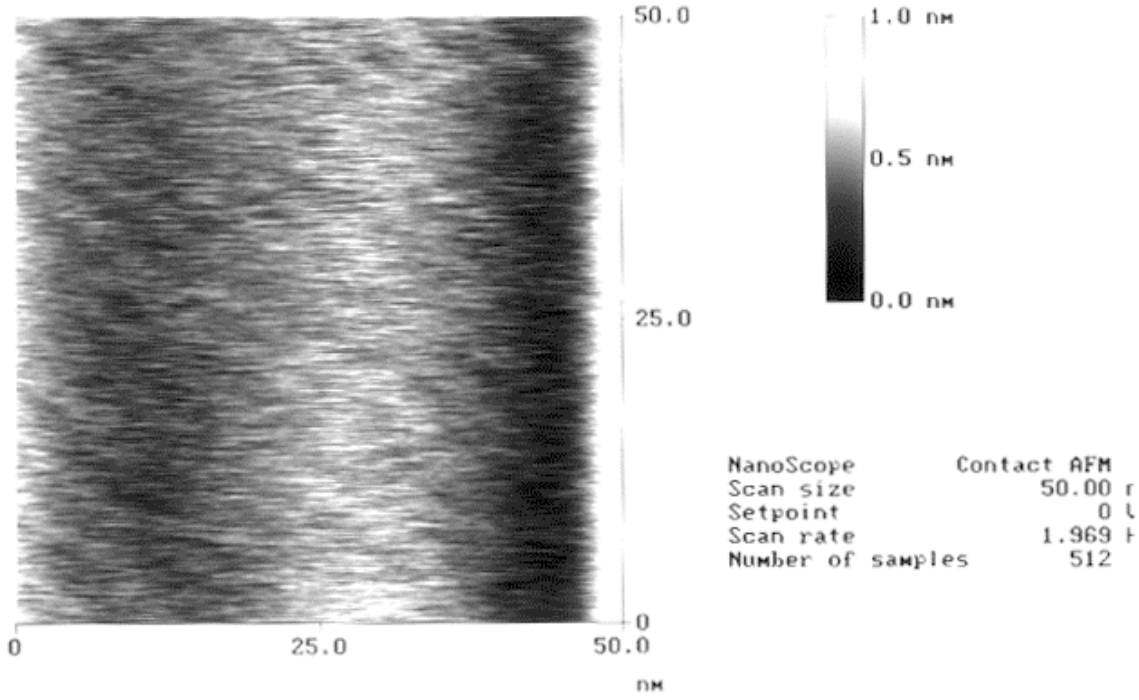

Figure 34: Scan of bicrystal of Figures 31-33, taken at a later time and in a different region

These images are promising but the question remains whether or not the surface structure is definitively linked to the structure of the buried grain boundary. The strong correlation between the peak spacing and dislocation spacing shown in **Figure 33** suggests that the two structures are related. The fact that the image was effectively reproduced in a different area of a the same specimen supports this conclusion. However, the strength of the pattern in one direction as opposed to its strength in the other introduces some doubt since a square periodicity is expected. Could the structure be a machine effect? Noise related to the frequency of an AFM scan is a frequent problem. However, looking in the lower or upper right of the upper image of **Figure 32** a series of very finely spaced lines can be seen. These lines are related to the frequency of the scan. In order to further validate the hypothesis that the periodic surface structure is due to the underlying grain boundary, scans were run, using exactly the same parameters as those of **Figures 32** and **33**, on a single crystal gold specimen and a silicon wafer. These images can be seen in **Figure 35 (a, b)**. Neither bears much resemblance to those acquired from the bicrystal. Based upon the evidence received so far, the simplest explanation for origin of the surface structure is the presence of the buried grain boundary.

The fact that the pattern is more obvious in one dimension than in the other still remains unexplained. Though strain energy will be reduced by the formation of a two dimensional periodic topography, such a process will produce excess surface area and thereby increase the energy of the system. Therefore, the surface that will form will be due to some equilibrium of these two energy terms. It may be possible that an essentially one-dimensional periodic surface structure is such a minimum

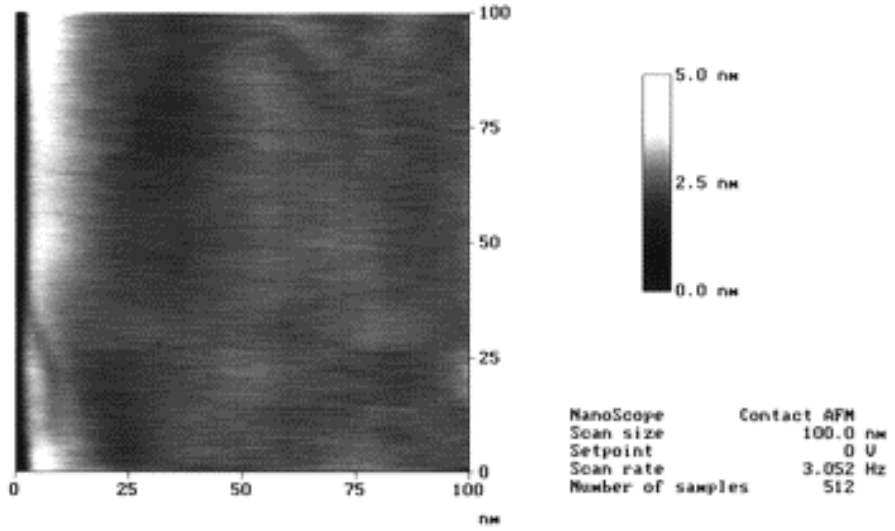

a) Gold Single Crystal Surface

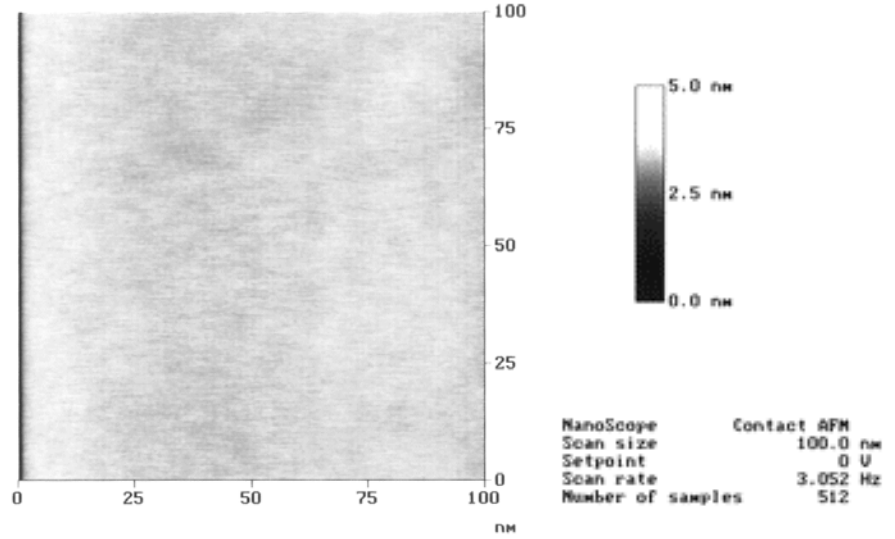

b) Silicon Single Crystal Surface

Figure 35: Gold and silicon single crystal surfaces, scans using same parameters as in Figure 32

energy configuration. The prior surface of the gold will also influence the final state. In addition to thermodynamic calculations, an exact determination of the most likely surface structure would also have to take into account kinetic considerations.

An additional gold bicrystal was prepared attempting to keep the misorientation angle as small as possible. **Figure 36** shows the SAD pattern of the resultant bicrystal while **Figure 37 a, b** shows the bright field image of the grain boundary. Only the diffraction spots far from the 000 reflection show measurable signs of splitting. From this pattern it was determined that the boundary was produced with a misorientation angle of less than 0.5°. According to Frank's Rule, the dislocation spacing of such a specimen should be 33 nm. As can be seen from **Figure 37**, the dislocation spacing varies dramatically across the specimen. Due to the metallic bonding and 'soft' nature of gold, dislocations have more freedom in a gold boundary. At the large spacings of 0.5° boundary, the dislocations may not interact all that strongly and adopt a configuration that is less than perfectly periodic.

Figure 38 shows an AFM scan of the surface of this bicrystal, taken with parameters similar to those used for the previous bicrystal. The pattern is very similar to that observed in **Figure 32**. The spacing of the peaks is only 6.9 nm, much smaller than the Frank's Rule calculated 33 nm. However, dislocation spacings as small as 9.8 nm have been measured in the images of **Figure 37**. It is not clear whether or not these surface structures can be linked to the buried grain boundary. **Figure 39** shows an AFM scan of another region of this specimen. A number of two-dimensional features are present in this image. The spacing of such hills is

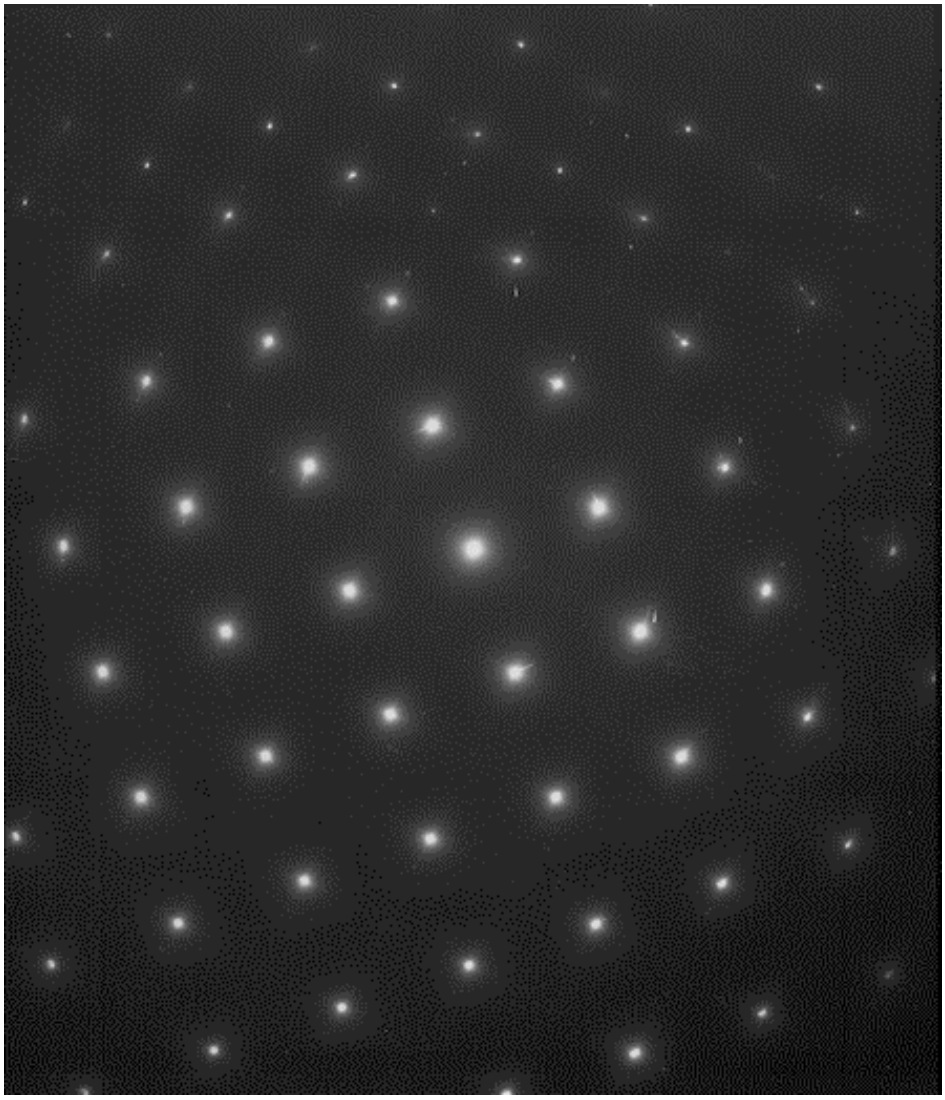

Figure 36: SAD pattern of very small angle Au twist boundary

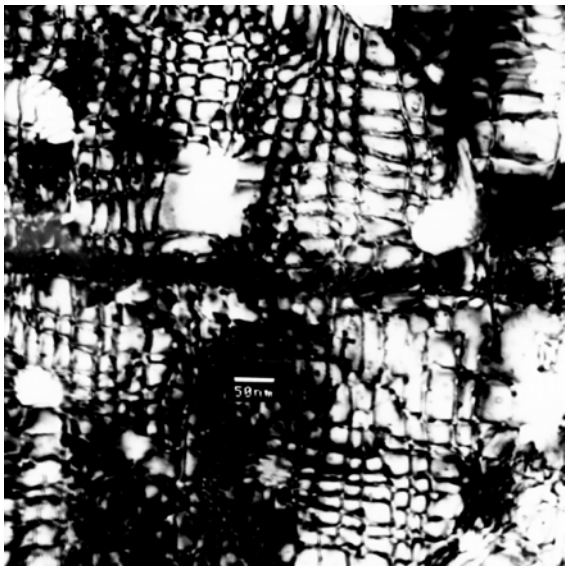

a) region exhibiting much variation in dislocation spacing

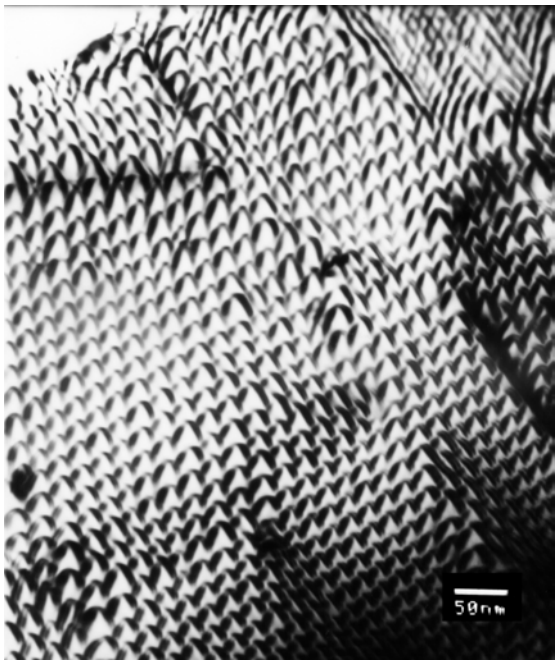

b) region exhibiting 'odd' dislocation geometry

Figure 37: Bright field images of very small angle Au twist boundary

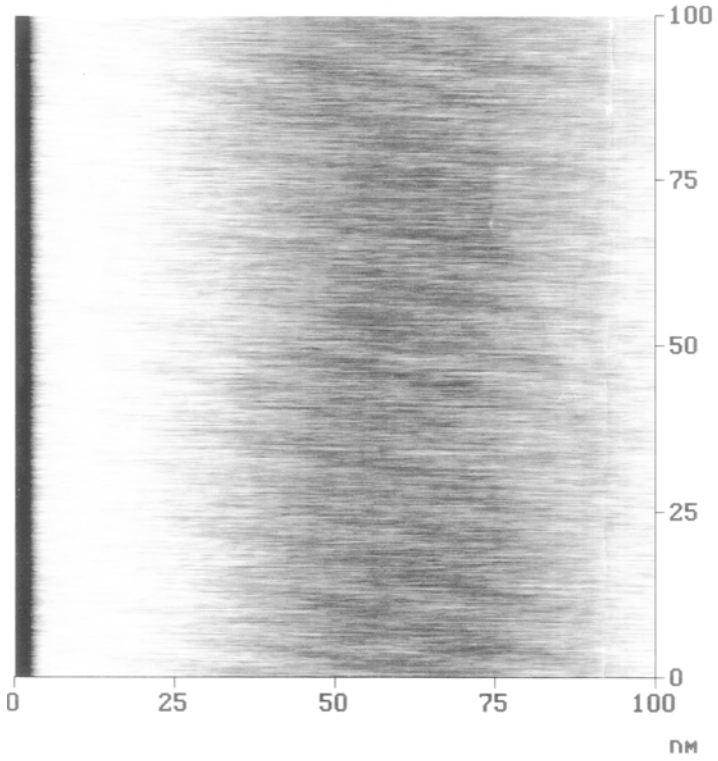

Figure 38: AFM scan of specimen seen in Figure 37

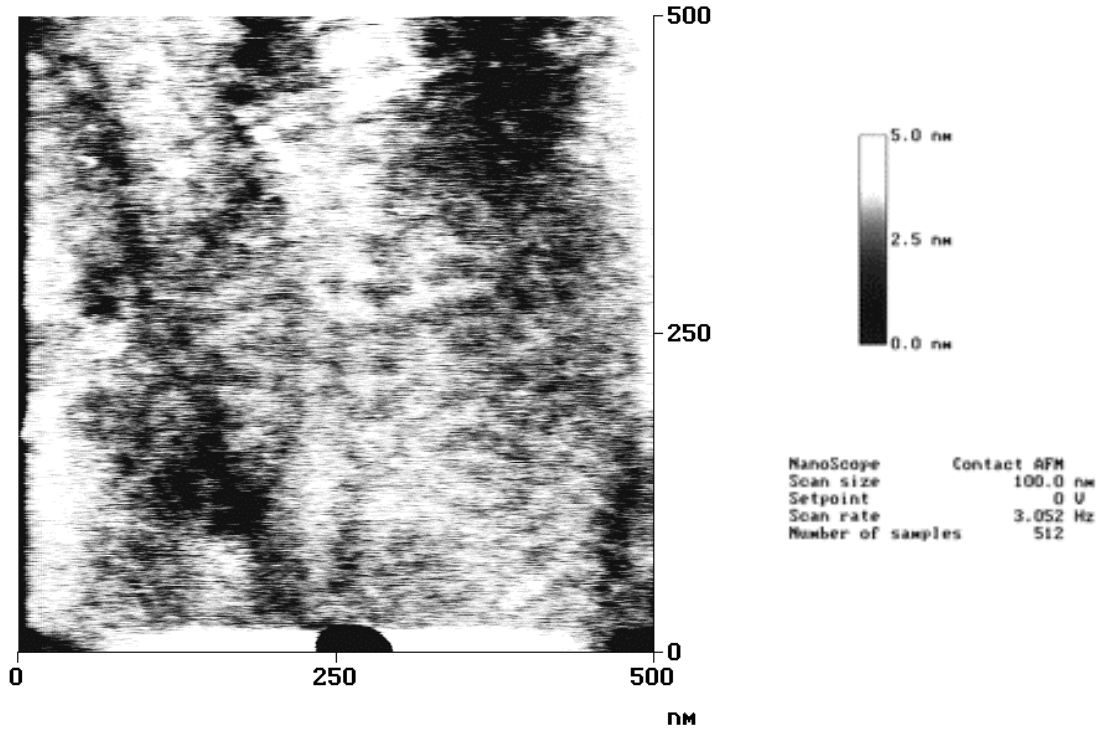

Figure 39: AFM scan of another region of the very small angle Au bicrystal

11 nm, far from the Frank's rule value for the dislocations of the boundary, but within the spacings observed in the TEM.

A 1.5° twist boundary specimen was also examined. Smaller angle boundaries have a larger dislocation spacing and, thus, their stress fields are appreciable over larger distances. It was hoped that a smaller angle bicrystal would yield a more appreciable variation in surface topography. These specimens were electron transparent without any ion milling, so it was known that they could be no more than a few hundred angstroms total thickness. The bright field TEM image of this specimen is presented in **Figure 40**. A dislocation array is still present but it is no longer perfectly periodic; it is 'sloppy'. Stress fields in the regions of such a boundary are exceedingly complicated and impossible to analytically calculate. **Figure 41** shows a high magnification AFM scan of the surface of this bicrystal. Some surface structures are visible however, there are no large domains of any one structure. The visible topography may be due to the underlying grain boundary, since its stress field is not perfectly periodic, however, no unequivocal conclusion can be drawn from this evidence.

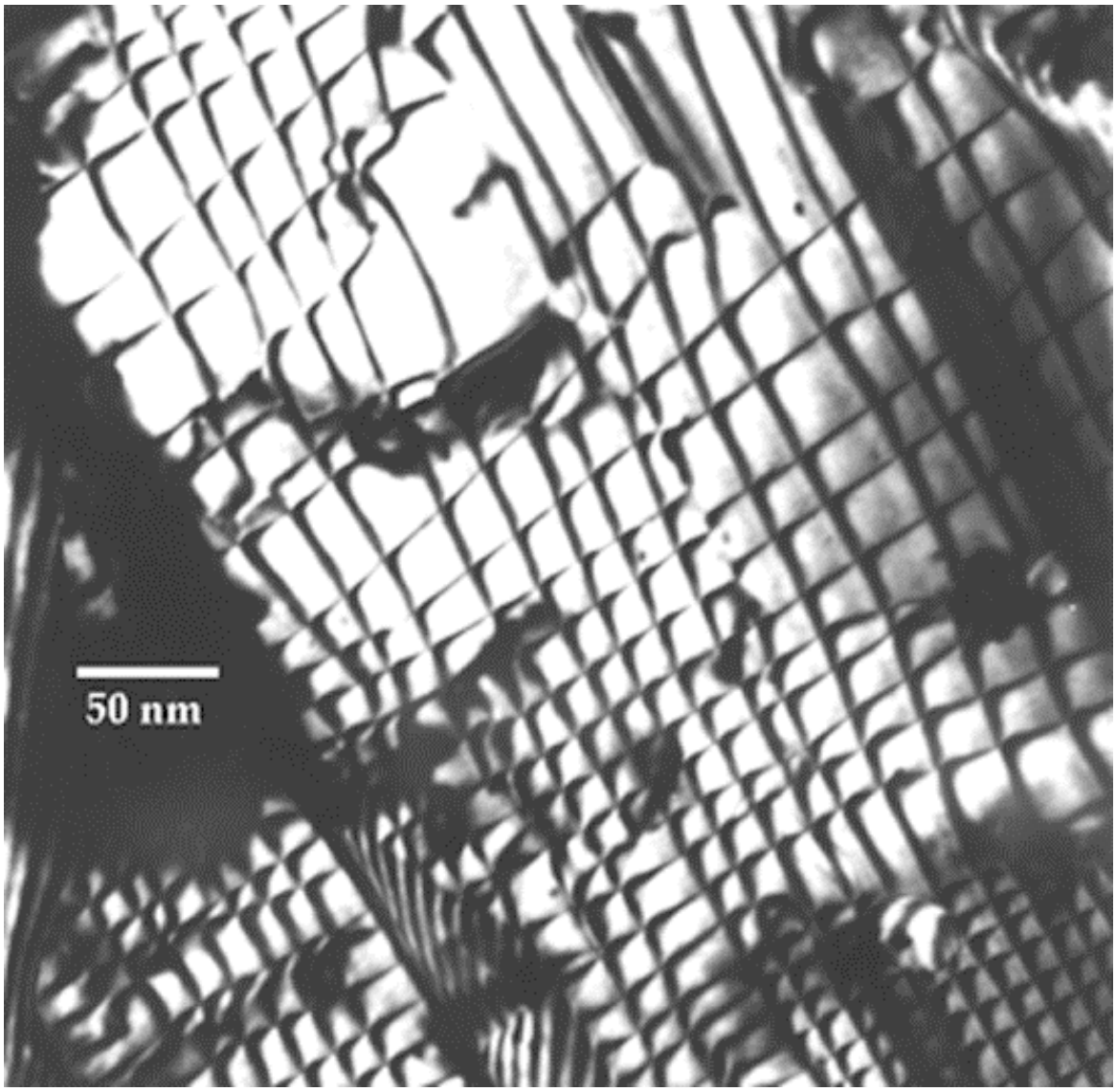

Figure 40: Bright field image of 1.5° twist boundary

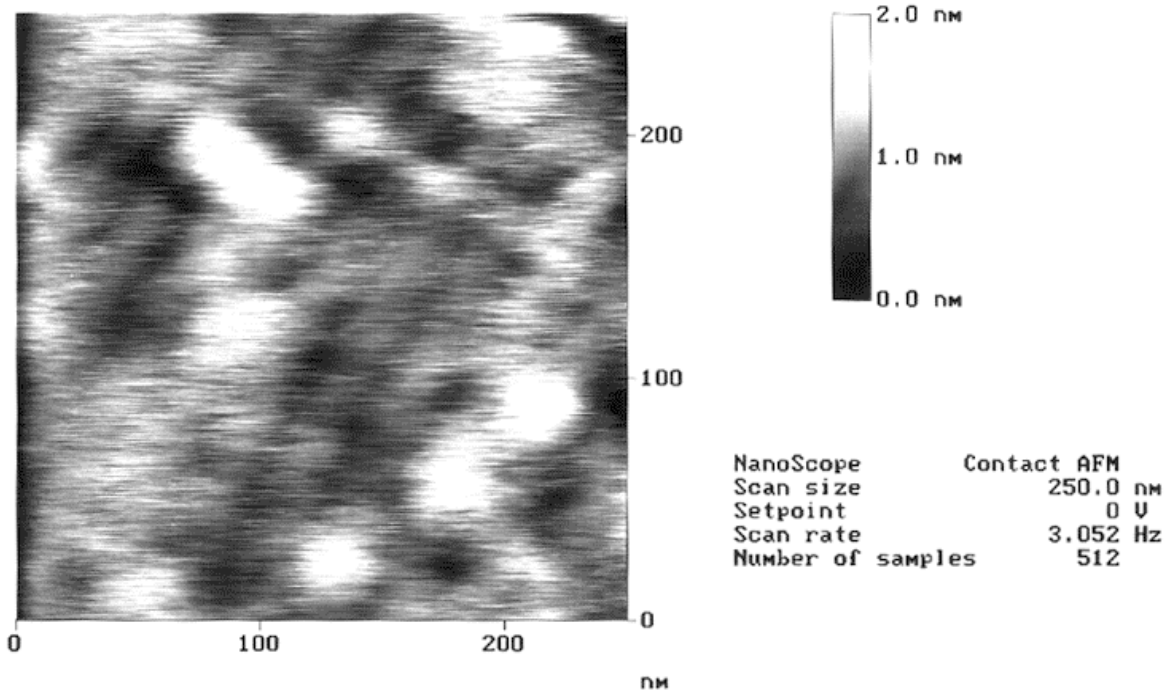

Figure 41: AFM scan of 1.5° bicrystal surface

CHAPTER FOUR:
SUMMARY

4.1 SUMMARY

Further evidence of the successful growth of lattice mismatched heteroepitaxial layers by the compliant universal substrate technique has been presented. Examination of a germanium film grown on a silicon compliant universal substrate, a 4% compressive mismatch, has shown a small defect density in a film ten times thicker than the Matthews-Blakeslee critical thickness. The compliant layer has been observed to migrate out of the film during processing. Defect density does vary greatly between regions containing a compliant layer and those without one. Structure has been observed at both types of interfaces. The structure related to the compliant layer appears to be roughly periodic. The earlier results on GaSb growth on a GaAs CUS now seem to represent those of a growth that occurred without the presence of a compliant layer.

Techniques for bonding silicon have been developed. Mechanically strong bonds were formed, although no direct observations of twist boundary structures were achieved. Annealing at 950°C in vacuum has been found to form an interfacial bond when the wafers are subjected to rigorous cleaning involving RCA cleaning followed by hydrogen termination of the surface. Much less stringent cleaning techniques can still be used to form interfacial bonds provided that the heat treatment is more extreme. Specimens that were ultrasonically cleaned in acetone and hydrogen terminated were found to bond when subjected to a 68 hour anneal at 1200°C in a low vacuum under a 3 MPa applied load.

Gold single crystals have been produced on sodium chloride substrates by sputter deposition at a substrate temperature of 450°C. The quality of such crystals was improved by a subsequent one hour anneal at 660°C. Gold bicrystals have been formed through hot pressing at 300°C for one hour under a 1 MPa applied pressure.

A periodic template structure with a 5 nanometer spacing has been formed on a gold bicrystal surface. This surface modulation was caused by the presence of an underlying 3.4° twist boundary and its accompanying stress field. The amplitude of these "hills" was found to be 0.5 nm. Examinations of Au single crystal surfaces and Si wafer surfaces revealed no structures similar to that seen on the bicrystal surface, thereby supporting that this effect is real and not a mere machine effect.

Examination of the surface of a 1.5° Au bicrystal and a <0.5° Au bicrystal proved less conclusive. Structures were found on the surface of the 1.5° bicrystal but they were far from being perfectly periodic. However, the dislocation structure of this grain boundary was found to have great variability and this accounts for the imperfect periodicity of the structures found. The surface of the <0.5° bicrystal showed structures having a one-dimensional periodicity similar to that of the 3.4° bicrystal and structures with a two-dimensional periodicity. The dislocation structure of this twist boundary was not perfectly periodic due to the small angle and, hence, it was difficult to coordinate the structure of the buried grain boundary and the surface.

4.2 FUTURE DIRECTIONS

Further characterization of the compliant substrate specimen is an obvious necessity. In particular, a high-resolution investigation of the compliant layer would be highly useful. This will provide the most insight into both the mechanism of compliance and the mechanism of migration. A series of trials on the new bonding device also must be carried out.

Replication of the periodic template results must be achieved. As was seen in Chapter 3, replication has been mildly successful at best. The fact that, after a few days, periodic surfaces have not been found on specimens which previously possessed them suggests that such structures may not be highly stable. A relaxation of strain may be occurring or they may be so fragile that casual handling is destroying them. Another possibility is that the surface structure is being buried under a 'dirt' layer of some sort.

Thorough calculations of the energetics related to the surface structure should be carried out. One can use the stress fields of Section 1.1.1 to calculate the strain energy profile. Some algorithm for the surface energy as function of deformation must then be developed. By establishing the minima of these two energies one can establish a likely surface profile. This may shed light onto the question of the one-dimensionality of the structures produced.

Finally, work should continue on the silicon periodic template. It is this author's opinion that a doped, silicon twist boundary, suitably etched, holds the strongest promise for a square, large-area periodic template with a useful height variation.

BIBLIOGRAPHY

[1] F. Ejeckham, Y-H Lo, S. Subramanian, H. Hou, B. Hammons. *Appl. Phys. Lett.* **70** (13), 31 March 1997. pp. 1685-1687.

[2] J. Hirth and J. Lothe. Theory of Dislocations. McGraw-Hill. New York. 1968.

[3] R. Reed-Hill, R. Abbaschian. Physical Metallurgy Principles. PWS-Kent. Boston. 1992.

[4] H. Baumgart, H. Leamy, L. Trimble, C. Doherty, G. Celler. Grain Boundaries in Semiconductors. MRS Symposia Proceedings. Pittsburgh. 1982. pp. 311-316.

[5] B. Pivac Polycrystalline Semiconductors. Springer-Verlag. New York. 1989. pp. 170-174.

[6] I. Delidais, D. Ballutaud, A. Boutry-Forveille, J. Maurice, A. Zozime, M. Aucouturier Polycrystalline Semiconductors II. Springer-Verlag. New York. 1991. pp. 200-204.

[7] K. Ahn, R. Stengl, T. Tan, U. Gosele, P. Smith. *J.Appl. Phys.* **62** (2) pp. 561-563.

[8] J. Van der Merwe. *Proc. Royal Soc.* **A63** 1950. p. 616

[9] R. E. Peierls. *Proc. Phys. Soc.* **52** 1940. p. 23

[10] F. R. N. Nabarro. *Proc. Phys. Soc.* **59** 1947. p. 256

[11] F. C. Frank and J. Van der Merwe. *Proc. Royal Soc.* **A198** 1949. p. 205

[12] F. C. Frank and J. Van der Merwe. *Proc. Royal Soc.* **A200** 1950. p. 125

[13] R. Sheally. Unpublished Lecture Notes. Cornell University. 1991.

[14] G. Agrawal and N. Dutta. Semiconductor Lasers. 2nd ed. Van Nostrand Reinhold. New York. 1993.

[15] J. Matthews and A. Blakeslee. *J. of Crystal Growth.* **27** 1974. pp. 118-125.

[16] J. Bean, J. Feldman, A. Fiory, S. Nakahara, andI. Robinson. *J. Vac. Sci. Technol*. 12 1975. pp. 436-440

[17] W. D. Nix. *Met. Trans. A.* **20A** 1989. pp. 2217-2245.

[18] W. Hagen and H. Strunk. *J. Appl. Phys*. **17** 1978. pp. 81-85

[19] Z. Liau and D. Mull. *Appl. Phys. Lett.* **56** (8) 1990. pp. 737-739

[20] R. Venkatasubramanian, M. Timmons, T. Humphreys, B. Keyes, and R. Ahrenkiel. *Appl. Phys. Lett.* **60** (7) 1992. pp. 886-888

[21] R. Ram, J. Dudley, J. Bowers, L. Yang, K. Carey, S. Rosner, and K. Nauka. *J. Appl. Phys*. **78** (6) 1995. pp. 4227-4237

[22] M. Kimura, K. Egami, M. Kanamori and T. Hamaguchi. *Appl. Phys. Lett.* **43** (3) 1983. pp. 263-265

[23] E. Yablonovitch, T. Gmitter, J. Harbison, and R. Bhat. *Appl. Phys. Lett.* **51** (26) 1987. pp. 2222-2224

[24] F. Ejeckham, Y-H Lo, S. Subramanian, H. Hou, B. Hammons. *Appl. Phys. Lett.* **70** (13), 31 March 1997. pp. 1685-1687.

[25] C. Carter-Coma, A. Brown, R. Bicknell-Tassius, N. Jokerst, and M. Allen. *Appl. Phys. Let.* **69** 1996. pp. 257-259

[26] C. Chua, W. Hsu, C. Lin, G. Christenson, Y. Lo. *Appl. Phys. Lett.* **64** (26) 1994. pp. 3640-3642

[27] F. Ejeckham. PhD. Dissertation. Cornell University. 1996.

[28] Shanthi Subramanian. Unpublished work. Cornell University. 1997.

[29] Cornell Nanofabrication Facility. User Procedures Manual. Cornell University. 1995.

[30] M. Fitzsimmons, E. Burkel, and S. Sass. *Phys. Rev. Lett.* **61** (9) 1988. pp. 2237-2240

[31] M. Fitzimmons. PhD. Dissertation. Cornell University. 1988.

[32] P. Lamarre. PhD. Dissertation. Cornell University. 1986.

[33] K. Milkove. PhD. Dissertation. Cornell University. 1984.

[34] R. Allen and P. Goodhew. *Acta Metallurgica.* **25** 1977. pp. 1095-1107

[35] L. Srivatsa and D. Crouse. private communication, Cornell University. 1998.